



Cephalopod proteins for bioinspired and sustainable biomaterials design

Iana Lychko^{a,b,1} , Inês Padrão^{a,b,1}, Afonso Vicente Eva^{a,b} ,
Catarina Alexandra Oliveira Domingos^{a,b} , Henrique Miguel Aljustrel da Costa^{a,b},
Ana Margarida Gonçalves Carvalho Dias^{a,b} , Ana Cecília Afonso Roque^{a,b,*}

^a UCIBIO – Applied Molecular Biosciences Unit, Department of Chemistry, School of Science and Technology, Universidade NOVA de Lisboa, 2829-516, Caparica, Portugal

^b Associate Laboratory I4HB – Institute for Health and Bioeconomy, School of Science and Technology, Universidade NOVA de Lisboa, 2829-516, Caparica, Portugal

ARTICLE INFO

Keywords:

Protein-based materials
Cephalopods
Reflectins
Histidine-binding proteins
Suckerins

ABSTRACT

Nature offers a boundless source of inspiration for designing bio-inspired technologies and advanced materials. Cephalopods, including octopuses, squids, and cuttlefish, exhibit remarkable biological adaptations, such as dynamic camouflage for predator evasion and communication, as well as robust prey-capturing tools, including beaks and sucker-ring teeth that operate under extreme mechanical stresses in aqueous environments. Central to these remarkable traits are structural proteins that serve as versatile polymeric materials. From a materials science perspective, proteins present unique opportunities due to their genetically encoded sequences, enabling access to a diversity of sequences and precise control over polymer composition and properties. This intrinsic programmability allows scalable, environmentally sustainable production through recombinant biotechnology, in contrast to petroleum-derived polymers. This review highlights recent advances in understanding cephalopod-specific proteins, emphasizing their potential for creating next-generation bioengineered materials and driving sustainable innovation in biomaterials science.

1. Introduction

From a materials science perspective, proteins – in particular structural proteins – can be seen as extremely interesting biopolymers composed by well-defined amino acid sequences controlled at the genetic level by a bottom-up approach. Thus, the final polymer composition and functional properties are genetically encoded, which represents an enormous advantage in terms of materials design. Host cells translate this genetic code *in vivo* into a polymeric protein sequence using a carbon source, enabling the production of desired biopolymers through recombinant, scalable biotechnological methods, which offer significant environmental benefits. In addition, protein biopolymers can be processed under mild conditions (usually taking advantage of their intrinsic self-assembling mechanisms) into a variety of structural and functional biodegradable materials. Thus, several biotech companies are currently producing recombinant structural proteins with applications in textiles, medicine and cosmetic applications. A recent in-depth review from Miserez and co-authors covers aspects related to the molecular design

and artificial production of protein-based biological materials [1].

Observing Nature is a source of inspiration to design and engineer advanced functional materials and develop bio-inspired technologies. Cephalopods, including octopuses, squids, and cuttlefish, are fascinating animals with peculiar properties. One of the most astonishing features is their camouflage ability, by modulating their colour and texture as a mechanism to hide from predators and to communicate [2]. Another interesting observation is that cephalopods are ferocious predators containing extremely strong beaks and sucker ring teeth with unprecedented robustness and flexibility, working under elevated shearing and compressive forces in aqueous environments [3]. It is fascinating that three cephalopod-specific families of proteins serve as the foundation for these materials, enabling a remarkable range of light-manipulating properties and prey-capturing abilities. Here, we focus our attention on these three protein families: reflectins involved in light manipulation and camouflage found typically in the skin, histidine-binding proteins found in beaks, and suckerins which are the sole components of sucker-ring teeth (Fig. 1). Reflectins are intrinsically disordered proteins

* Corresponding author. UCIBIO – Applied Molecular Biosciences Unit, Department of Chemistry, School of Science and Technology, Universidade NOVA de Lisboa, 2829-516 Caparica, Portugal.

E-mail address: cecilia.roque@fct.unl.pt (A.C.A. Roque).

¹ Authors contributed equally.

<https://doi.org/10.1016/j.mtbio.2025.101644>

Received 23 January 2025; Received in revised form 4 March 2025; Accepted 6 March 2025

Available online 8 March 2025

2590-0064/© 2025 The Author(s). Published by Elsevier Ltd. This is an open access article under the CC BY-NC license (<http://creativecommons.org/licenses/by-nc/4.0/>).

(IDPs) that self-assemble into aggregated nanostructures that further organize into platelets and beads. *In vitro*, reflectin-based materials have shown light modulating properties and proton conductivity, with applications ranging from electronics to tissue engineering. In the beak, histidine-binding proteins (HBPs) form coacervates that infiltrate the chitin-fiber network and provide hardness to the whole structure. HBPs and derived peptides, with their ability to form coacervates, have been explored as efficient delivery systems, rivalling with existing

commercially available vehicles. In the sucker ring teeth, suckerin proteins self-assemble into robust supramolecular structures that form a semicrystalline polymer, reinforced by nano-confined β -sheets, resulting in a network with mechanical properties comparable with those of the strongest engineered polymers. Suckerin-based materials present interesting properties, such as glass-to-rubber transition, antibacterial activity, conductive properties, and modulated toughness, giving rise to a wide variety of applications.

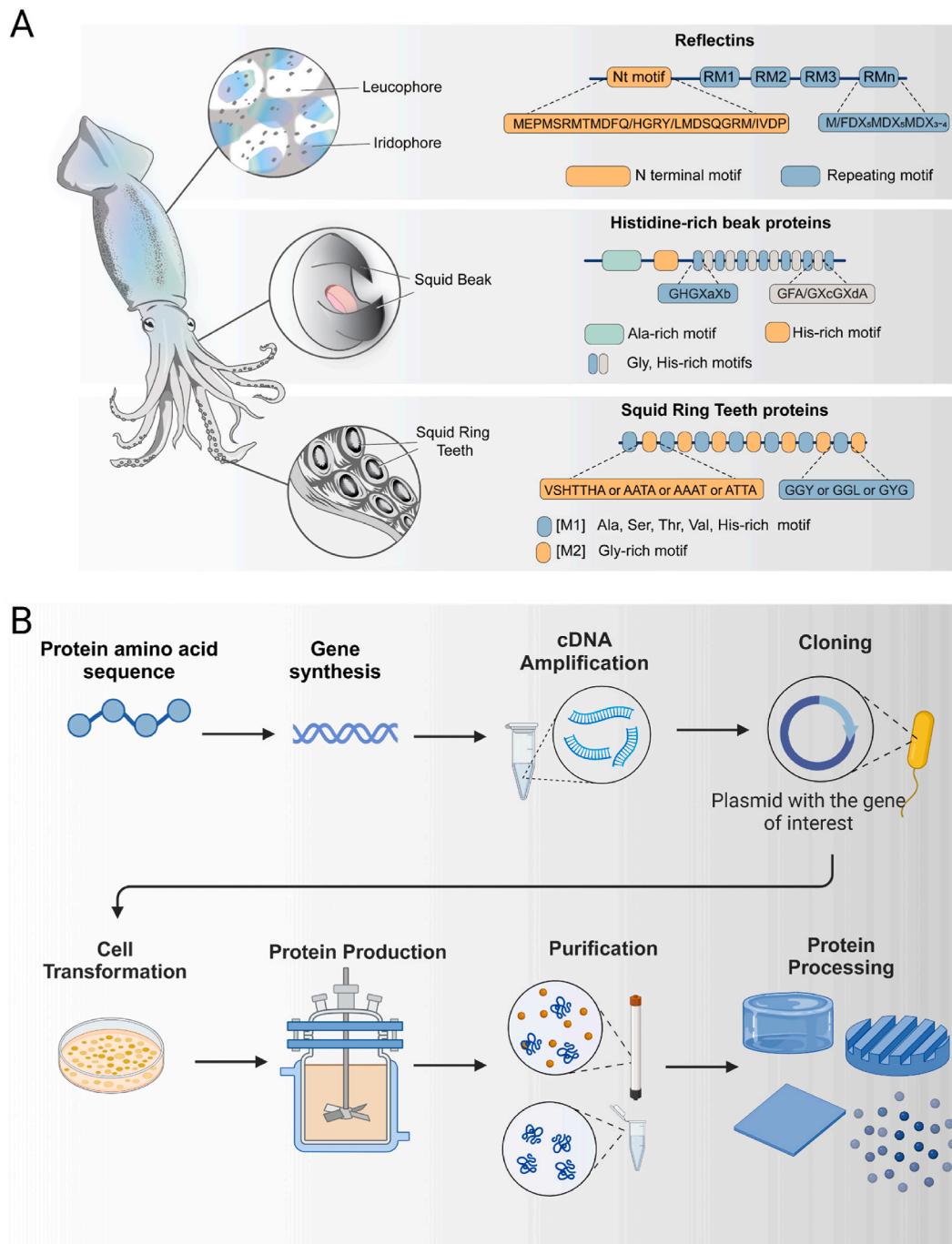


Fig. 1. Structural and functional insights of cephalopod proteins, their biotechnological production and processing into biomaterials. (A) Cephalopod proteins and their structural features. Reflectins, found in leucophores and iridophores, are important for light reflection and structural coloration. Histidine-rich beak proteins, present in squid beaks, feature Ala-rich, His-rich, and Gly/His-rich motifs that contribute to mechanical strength and rigidity. Squid ring teeth (SRT) proteins, located in the suction cup, contain His-rich (M1) and Gly-rich (M2) motifs, providing toughness and elasticity. (B) Biotechnological production workflow for cephalopod proteins. Genes coding for wild-type or engineered protein sequences are cloned into DNA expression vectors, transformed into bacterial hosts, and expressed in nutrient-rich media. The resulting proteins are purified and processed into functional materials. Created in BioRender. Roque, C. (2025) <https://BioRender.com/r11f005>.

This review explores the biological roles of reflectins, HBPs, and suckerins, emphasizing both wild-type and engineered proteins, as well as derived peptides, along with their structure-function relationships. We will discuss how these sequences are processed into advanced functional materials, their applications, and the future potential of engineering cephalopod proteins for materials science.

2. Reflectins and inspired materials

2.1. The biological context of reflectins

Cephalopods present an extraordinary dermal architecture that plays a crucial role in their ability to manipulate light and rapidly adjust their coloration [4]. The dermal layer of cephalopods has three main types of specialized organs and cells: chromatophores, iridophores, and leucophores as depicted in Fig. 2A. The synergy between these three layers enables remarkable dynamic coloration through light absorption, transmission, and reflection. As a result, cephalopods can change their patterns and tune structural color across a wide spectrum of visible light [5–8].

The top layer of cephalopod skin contains thousands of absorptive chromatophore organs that are filled with pigment granules of red, yellow, and brown colors. These chromatophores are connected to the radial muscles that, through their contraction and dilatation, control the exposure to the incident light area of the pigmented sac [5,6]. Beneath the chromatophores, there are two layers of light-reflecting cells: iridophores and leucophores. Differently from chromatophores that produce structural color due to the presence of pigments, iridophores and leucophores manipulate incident light through higher-order assemblies. Both types of cells contain protein-based insoluble moieties (e.g.

platelets or beads) with a higher refractive index in comparison to the refractive index of the surrounding cellular structures [7,9,10]. These insoluble structures are primarily composed of proteins from the unique family of cephalopod-proteins known as reflectins, that self-assemble into such remarkable architectures [9].

Inside iridophores, reflectins form multilayer structures of insoluble protein-based platelets alternated with the extracellular matrix [11]. The high concentration of reflectins in the platelets (estimated at 380 mg/mL [11] and about 18 % of the total dry weight of the dermal iridocytes [12]) contributes to a higher refractive index (1.44–1.51) in comparison to the extracellular space (1.35 ± 0.03) [13]. Such periodic arrangements create a natural Bragg reflector that, through thin-film interference phenomena, can create the iridescence colors of the entire visible spectra [14,15]. Cephalopods tune their structural coloration through the variation of the platelets thickness and the distance between them, through a process mediated by the neurotransmitter Acetylcholine (ACh) [12,16]. The release of ACh activates the enzymes responsible for the site-specific phosphorylation of reflectins [12] (tyrosine, serine and histidine side chains) and causes the neutralization of reflectins positive charge [11,16]. As a consequence, charge repulsion between reflectin particles decreases, leading to condensation [11,15], that causes a shrinking of the protein platelets and reduction of the distance between them, thus altering the thickness of the Bragg reflector layers and the specular reflection of the incident light with different wavelengths and intensities.

Regarding leucophores, reflectins are one of the constituents found within spherical microparticles (leucosomes) that constitute leucophores [10]. The random distribution of polydisperse leucosomes induces the scattered reflection of the incident light in all directions in an angle-independent manner. Leucophores dynamically control the

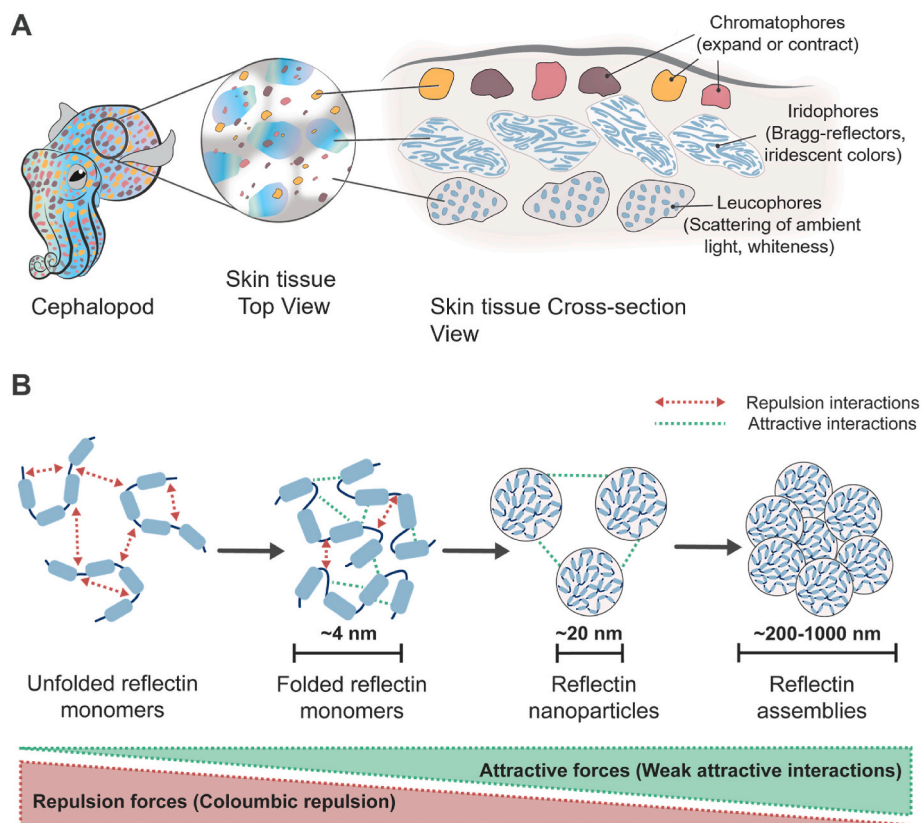


Fig. 2. Illustration of the cephalopod skin structure and reflectin self-assembly. (A) Cross-sectional schematic of the dermal layer, highlighting chromatophores with pigment granules, followed by iridophores and leucophores, which enable dynamic camouflage. (B) Depiction of the hierarchical self-assembly of reflectin proteins, where charge interactions regulate the transition from monomers (~4 nm) to nanoparticles (~20 nm) and ultimately into higher-order structures (<1000 nm). Under physiological conditions (pH ~7.0), Coulombic repulsions keep monomers dispersed, while charge neutralization reduces repulsion, allowing attractive forces to drive self-organization into structured assemblies.

transparency of the cephalopods and function as white Lambertian surfaces, exhibiting broad-band reflectance and light diffusion [6,10,13].

Besides cephalopods' skin tissue, reflectin-based platelets can be found in reflective tissues of the eye and light organ reflector (LOR) where they are also arranged in insoluble platelets [17,18]. More recently, reflectins were also identified as a structural constituent within pigment granules of chromatophores in *Sepia officinalis* [19]. It is suggested that their presence in chromatophores enhances the optical properties of their granules contributing to the animals' rapid adaptation.

2.2. Reflectins organization and assembly

Reflectins are intrinsically disordered proteins (IDPs) which can be organized in two types – canonical and non-canonical sequences.

Overall, reflectin sequences present a deficiency in bulky hydrophobic amino acids (<2.0 %), such as leucine, isoleucine, and valine, which are essential for forming compact folds and stable canonical secondary structures. On the other hand, reflectins are notably abundant in charged amino acids (>35 %), that increase the disorder conformation due to strong intrachain electrostatic repulsions. There is also a high content of methionine, arginine and tyrosine residues, important to establish weak inter- and intra-chain interactions involved in the self-assembly process. Furthermore, the substantial presence of highly polarizable residues, including phenylalanine, histidine, methionine, tyrosine, arginine, and tryptophan, contributes significantly to a high refractive of reflectin-based structures (dn/dc) [20].

So far, canonical sequences have been the most widely studied, and the typical modular sequence comprises several conserved Repeating Motifs (RMs: MDX₅(MDX₅)_nMDX₃₋₄, where X = S, Y, Q, W, H, R) and a highly conserved N-terminal domain (N-term: MEPMSRMTMDFQ/

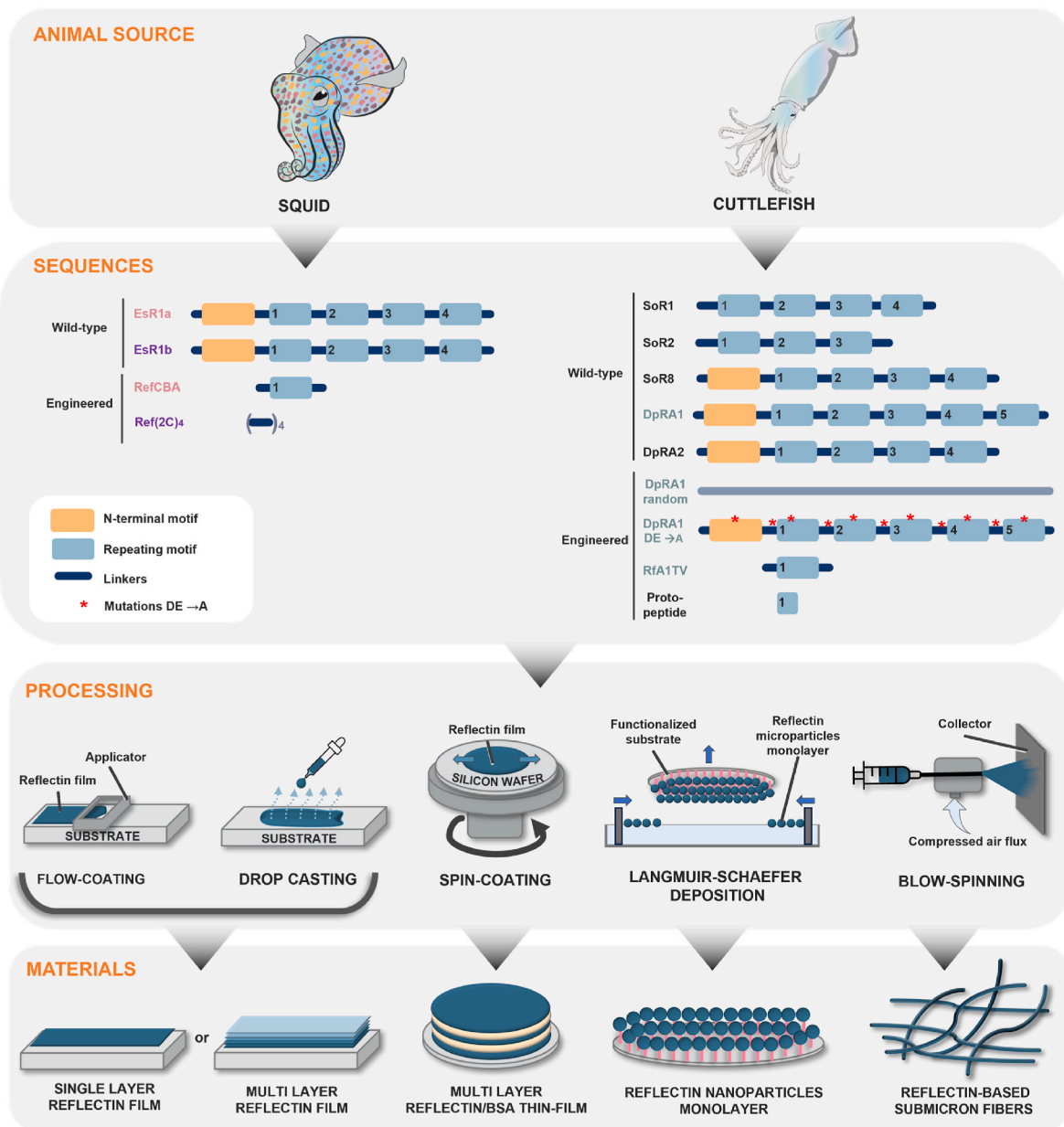


Fig. 3. Overview of the pathway from natural reflectins to functional materials. Reflectins derived from squids and cuttlefishes are categorized into wild-type and engineered sequences, including variants, e.g. RefCBA, Ref(2C)₄, and DpRA1 with specific mutations. These proteins undergo various processing techniques to form diverse materials.

HGRY/LMDSQGRM/IVDP), all connected by linkers as shown in Figs. 1A and 3. Linkers are much more variable in composition and length in comparison to RMs and show a cationic nature since they are enriched in arginine and histidine residues.

The capacity of reflectin nanoparticles to self-assemble is one of the secrets to both their ability to organize into higher-order structures in biological systems and their capacity to form advanced functional materials. The exact *in vivo* mechanism by which the formation of reflectin-based ultrastructures remains unknown up to the present day. Nonetheless, the combination of *in vitro* and *in silico* studies have been contributing to understand reflectins self-assembly mechanism and to understand how it can be reconfigured *in vitro*, as further explained.

Levenson and colleagues used full-length reflectins (A1, A2, B, and C) from *Loligo opalescens* and a series of reflectin A1-based mutants, to study how self-assembly varies upon modification of proteins' net charge as a surrogate of phosphorylation [21,22]. The authors correlated the net charge density of the cationic linkers and the final size of the reflectin nanoparticles, with a lower net charge leading to the formation of larger nanoparticles. Moreover, they showed that the driving force that triggers the structural transition upon charge neutralization is

spatially distributed within the cationic linkers along the protein's sequence instead of being confined to a specific position [15,21–23]. These results have been further detailed on a colloidal model of the pH-modulated self-assembly of reflectin A1 and liquid-liquid phase separation at high pH (LLPS) [24]. Recently, Lychko and co-workers studied the kinetics of charge-dependent reversible condensation of reflectin nanostructures, highlighting the effect of protein sequence on the remarkably fast and steady reversible condensation of reflectin nano and microstructures as a function of pH [25]. Fig. 2B schematically represents the hierarchical self-assembly of reflectins, summarizing the key processes and correlations observed in these studies.

2.3. Reflectin-based materials

Reflectins were first reported in the squid *Euprymna scolopes* by Crookes and colleagues in 2004 [9], and since then several advanced materials and biomimetic technologies arose [15,17,18,26]. Over the past 20 years, a multitude of reflectin sequences have been isolated from other species of squids [27–30], cuttlefish [31,32], and octopuses [33], with a particular emphasis on proteins from squids and cuttlefishes,

Table 1

Wild-type reflectin sequences used to produce bio-based materials. The table includes the key features of the protein sequences and the resulting materials as well as potential applications of these materials.

Protein name /Uniprot ID	Species	MW (kDa)	pI	Key features	Applications	Ref
Reflectin 1a (R1a)/ Q6WDN8	<i>Euprymna scolopes</i>	^{a)} 36.7	^{a)} 8.84	Reflectin-based films show reversible color changes with humidity fluctuations. Reflectin-based fibers lack crystallinity	Optical & stimuli-responsive: production of stimuli-responsive photonic biopolymer.	[28]
Reflectin 1b (R1b)/ Q6WDN7	<i>Euprymna scolopes</i>	38.0	8.92	Light scattering changes result from reflectins self-assembling into micro- and nanoscale structures in response to stimuli.	Optical & stimuli-responsive: materials with stimuli-induced light scattering	[47]
Reflectin A1 (RA1)/ D3UA43	<i>Doryteuthis (Loligo) pealeii</i>	44.6	9.06	Reflectin-based films exhibit reversible color changes in response to humidity, mechanical stress, and acidity. Reflectin-based films with proton conductivity of $\sim 2.6 \times 10^{-3} \text{ S cm}^{-1}$, a proton transport activation energy of $\sim 0.2 \text{ eV}$ and proton mobility of $\sim 7 \times 10^{-3} \text{ cm}^2 \text{ V}^{-1} \text{ s}^{-1}$ Injecting or extracting protons directly into the reflectin-based layer alters its thickness, leading to observable shifts in reflectance spectra and coloration. R1A films facilitate the adhesion, proliferation, and differentiation of the hNSPCs The introduction of reflectin into human cells affected their optical properties (i.e., refractive index, light scattering) Amorphous photonic crystals (APCs) coated with reflectin were responsive to the acid stimuli in the NIR region.	Optical & stimuli-responsive: biomimetic chemically and mechanically modulated infrared camouflage coating. Ionic conductors: development of organic and biological protonic transistors. Bio-base photochromic devices: coloration changes in response to proton flow. Effective substrate for the growth and differentiation of cells. Optical engineering of mammalian cells: incorporation of reflectins into cells to tune their optical properties (i.e., refractive index and light scattering). Responsive coatings: coating with reflectin to incorporate stimuli-responsive properties.	[17, 34] [36, 41, 45] [26] [46] [48, 49] [44]
Reflectin A2/ D3UA44	<i>Doryteuthis (Loligo) pealeii</i>	29.1 28.3	9.02	RefA2-based materials showed proton conductivity between $4.3 \times 10^{-5} \text{ S cm}^{-1}$ and $7.4 \times 10^{-5} \text{ S cm}^{-1}$ Inside human cells RA2 creates diverse nanostructures, like nanoparticles and ribbon-like forms, maintaining consistent refractive indices across environments.	Ionic conductors: development of organic and biological protonic transistors Cellular optical engineering: Integrating reflectins to adjust cell properties like refractive index and light scattering. Optical reporters: Monitoring cell events like growth or division. Responsive optical coating: coating with reflectin to incorporate stimuli-responsive properties.	[38] [40]
Reflectin 1 (R1)/ IOJGV0	<i>Sepia officinalis</i>	^{a)} 35.6	^{a)} 8.92	All three reflectins self-assemble into higher order structures.		
Reflectin 2 (R3)/ IOJGV1	<i>Sepia officinalis</i>	^{a)} 31.8	^{a)} 8.60	Processed reflectins form thin films with structural blue color that changes with humidity levels.		
Reflectin 8 (R8)/ IOJGV7	<i>Sepia officinalis</i>	^{a)} 37.6	^{a)} 8.85			
Reflectin B1/ ^{b)} NA	<i>Septeuthis lessoniana</i>	^{a)} 30.8	^{a)} 8.89	Precise control of the reflectin-based assemblies through modulation of hydrophobic interactions. Tunable coloration in reflectin-based thin films based on particle size.	Optical & stimuli-responsive: reflectin-based coating with tunable structural colors that mimic cephalopods' dynamic camouflage.	[29]

^a Indicates that the MW and pI were not reported in the literature and were calculated using the Prot/Param tool on the EXPASY server. As an input, it was used the sequence reported in the corresponding reference or protein sequence available in the database without the histidine tag.

^b NA – Not available.

which have been the most studied and explored for biomimetic materials (Fig. 3). Several research teams use full-length, wild-type as well as engineered versions of reflectins to produce protein-based materials [17, 28,34,35]. In the next sections, we summarize the works regarding the processing and use of reflectins (Table 1) and engineered versions (Table 2) in materials science.

Reflectin proteins and peptides can undergo various treatments using distinct processing techniques, such as flow-coating [28], spin-coating [35], drop-casting [36], Langmuir-Schaefer deposition [29], and blow-spinning [37], resulting on a variety of materials, from single and multi-layer films, to reflectin nanoparticles monolayers and fibers (Fig. 3). The resulting materials, more specifically thin-films, show promising optical and proton conductivity properties [18,38,39] which are considered to be intrinsic to the unusual primary reflectin sequence [40,41]. Reflectin-based films displayed responsiveness to applied physicochemical stimuli, such as solvent vapors (e.g. water and acetic acid), proton injection/extraction or mechanical stretch [38,42,43].

2.3.1. Materials based on wild type reflectin sequences

Inspired by the natural function of reflectins, Kramer and colleagues were the first to recombinantly produce a reflectin protein from *Euprymna scolopes*. The produced protein was further processed into a variety of materials such as diffraction gratings, reflectin-based thin films, and fibers. Notably, thin films exhibited optical properties reversibly tuned through vapor-induced manipulations as shown in Fig. 4A [28].

As genetic information from various cephalopod species became accessible, different reflectin protein sequences were found. Cai et al. used reflectins from *Sepia officinalis* (reflectin 1, reflectin 2, and reflectin 8) to recreate *in vitro* the dynamic and reversible color changes observed on animal skin. Films with structural white and blue colors that turn colorless upon film hydration were produced by spin-coating [31]. Similar work was conducted by Wolde-Michael and colleagues, as full-length reflectin sequences from *Euprymna scolopes*, *Sepia officinalis*, and *Doryteuthis pealeii* were used to create single-layer thin films with angle-dependent optical signals over the wide spectrum range (UV–Vis–NIR) [35]. The authors also described the production of a biomimetic reflectin-based Bragg reflector, by spin-coating alternative layers of reflectin and bovine serum albumin (BSA). Due to such periodic architecture, the obtained films showed lower angle-dependent optical

properties [35].

Recently, a different approach was taken to obtain films with structural color. Low-polydisperse reflectin nanoparticles were produced by colloidal chemistry using full-length reflectin B1 from *Sepio-teuthis lessoniana*. Here, through hydrophobic interactions modulation, it was possible to precisely control reflectin nanoparticles size from 170 to 1000 nm. This modulation was achieved by adjusting solvent polarity which stabilized the hydrophobic regions of reflectin during the self-assembly process. A monolayer of reflectin nanoparticles with different dimensions were then immobilised by click chemistry onto azide-functionalized wafer substrates. The resultant films demonstrate variable structural colors dependent on the size of the nanoparticles used (Fig. 4A) [29].

Apart from the applications of reflectin-films for optical phenomena in the visible range, several examples extended to the development of biomimetic camouflage coatings within the infrared wavelength range. Phan and colleagues used reflectin A1 from *Doryteuthis pealeii* to develop a dynamic and stimuli-responsive reflectin-based coating whose optical properties could be tuned between visible and infrared wavelengths (400–1200 nm) as represented in Fig. 4B [34]. It has been demonstrated that the films' thickness varies in response to specific stimuli, such as acetic acid vapor, undergoing reversible swelling upon exposure to the vapor [17]. This variation alters the refractive index of the bio-based material, consequently inducing shifts in light reflectance spectra—shrinking resulting in a blue shift, while swelling leads to redshifts. Additionally, authors showed that coatings can be equally deposited on rigid (e.g. a silicon wafer, glass slide) [34] and flexible [17] substrates (e.g. FET tape) increasing the number of possible reflectins' applications.

Reflectins' capacity for stimuli-responsiveness has valuable applications in the sensing field and can be combined with other types of materials. Thus, Wang et al. used full-length reflectin A1 from *Doryteuthis pealeii* to coat inorganic particles, recognized for their role as photonic crystals. Their study revealed that films comprising these reflectin-coated particles exhibited enhanced and reversible responsiveness to acidic environments. This responsiveness was characterized by notable shifts observed in the reflectance spectra [44].

In addition to optical characteristics, reflectin-based materials exhibit impressive electrical properties, particularly in terms of proton conductivity, comparable with non-protein biomolecules [38,43,45].

Table 2

Engineered reflectin sequences and reflectin-based peptide sequences used for production of bio-based materials. The table includes the key features of the protein sequences and the resulting materials as well as potential applications of these materials.

Protein name	Species	MW (kDa)	pI	Key features	Applications	Ref
Reflectin 1A	<i>Doryteuthis (Loligo) pealeii</i>	43.0 (DE→A) 44.6 (Random)	^{a)} 9.06 (WT)	Proton conductivity of reflectin-based materials can be modulated through variation of the amount of polar charged residues.	Ionic conductors: development of organic and biological protonic transistors with tunable conductivity.	[36]
RefCBA	<i>Euprymna scolopes</i>	~14.0	^{a)} 5.07	RefCBA-based films with different thicknesses and structural colors	Optical & stimuli-responsive: photonic biopolymer that responds to humidity variations.	[30]
Ref (2C) ₄	<i>Euprymna scolopes</i>	15.7	7.87 8.89	Minimal region of reflectin sequences that can recapitulate the light scattering properties observed in thin films of the full-length protein. Ref(2C) ₄ -based device showed proton conductivities with values of ~0.4 mS cm ⁻¹ and sustained proton transport over distances of ~1 mm.	Optical: materials with stimuli-induced light scattering Long-range ionic conductors: development of peptide-based protonic transistors.	[47] [39]
Reflectin A1 truncated variant (RfA1TV)	<i>Doryteuthis (Loligo) pealeii</i>	7.8	5.77	Mechanical agitation alters RfA1TV peptide folding, that directly impacts the architecture of RfA1TV-based higher-order structures and refractive index distribution.	Self-Assembly: RfA1TV forms diverse structures (nanoparticles, fibrils, beads-on-a-noodle) via mechanical agitation. Optical properties: Different RfA1TV architectures exhibit varied refractive index distributions.	[51]
Protopeptide	A common motif in reflectin sequences	0.99	3.7	Protopeptide demonstrates the ability to self-assemble into higher-order structures and can be processed into submicron fibers, hydrogels, and films.	Self-assembly: modulation of fiber assembly through solvent variation	[37, 53]

^a Indicates that the MW and pI were not reported in the literature and were calculated using the Prot/Param tool on the EXPASY server. As an input, it was used the sequence reported in the corresponding reference or protein sequence available in the database without the histidine tag.

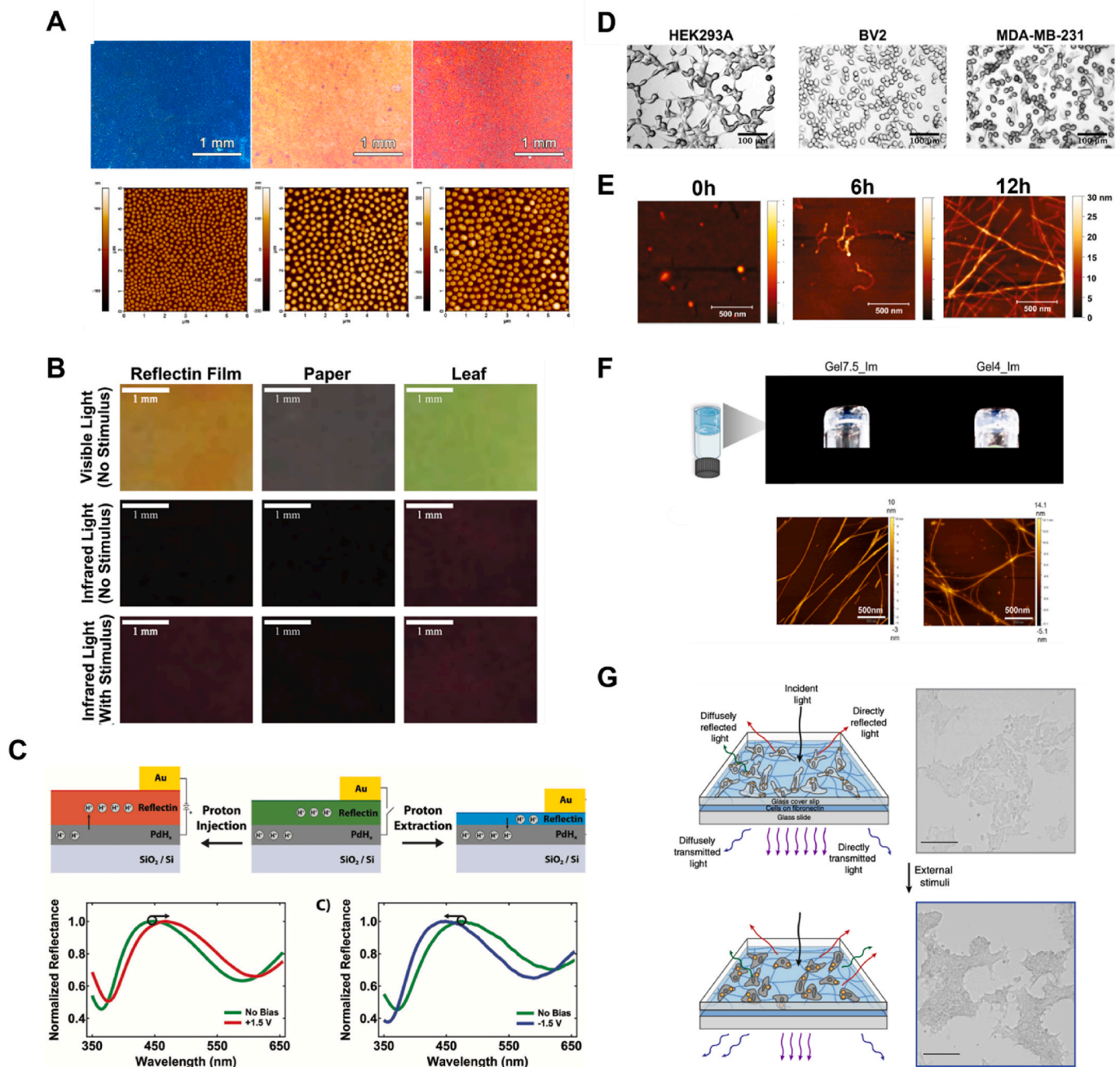


Fig. 4. Examples of the processing and applications of reflectin-based materials. (A) Structural coloration of DBCO-SIRF-B1 reflectin nanoparticle monolayers deposited via Langmuir–Schaefer, shown in, top row, light microscopy and, bottom row, AFM images. Reproduced with permission [29]. Copyright 2025, American Chemical Society. (B) Infrared camouflage coatings using reflectin proteins, shifting appearance under acetic acid vapor. Reproduced with permission [34]. Copyright 2025, John Wiley and Sons. (C) Proton injection/extraction effects on reflectin film thickness and reflectance in a sandwich-like device architecture. Reproduced with permission [26]. Copyright 2025, John Wiley and Sons. (D) Microscopy images showing adhesion of different mammalian cells on reflectin films. Reproduced under terms of the CC-BY license [46]. Copyright 2025, Phan et al., published by American Chemical Society. (E) AFM analysis of RfA1TV peptide assembly under mechanical agitation over time. Reproduced under terms of the CC-BY license [51]. Copyright 2025, Umerani, M et al., published by National Academy of Sciences. (F) Self-assembled protopeptide-based hydrogels at different pH conditions. Reproduced under terms of the CC-BY license [53]. Copyright 2025, Dias et al., published by Frontiers Media S.A. (G) Engineered reflectin-expressing human cells altering light attenuation under varying NaCl concentrations. The scale bars are 225 μm. Reproduced under terms of the CC-BY license [49]. Copyright 2025, Chatterjee, A. et al., published by Springer Nature.

Full-length reflectins A1 and A2 (wild-type or histidine-tagged) from *Doryteuthis pealeii* were used to fabricate protein-based protonic transistors with similar properties [38,43]. Research demonstrated that two key components with significant influence on electrical responses of the reflectin-based active layer are: environmental humidity conditions and the electrodes used [36,45]. Consequently, to increase proton conductivity it is preferable to maintain higher humidity levels to increase the

formation of hydrogen-bonded pathways for proton transport and use electrodes that facilitate direct proton injection (e.g. palladium hydride (PdHx)) [26,36,43]. Additionally, Phan et al. showed that through direct injection or extraction of protons, it is possible to achieve dynamic variation of optical properties of a reflectin-based active layer [26]. As highlighted in Fig. 4C these variations manifest as changes in structural color and shifts in reflectance spectra. Research into the impact of

protein sequence composition has also uncovered the significant role of residues featuring carboxylic acid side chains (such as glutamic and aspartic acids) in modulating protonic conductivity [26]. It has been postulated that these amino acid residues may serve as proton donors or facilitate more efficient proton transport. Indeed, studies have demonstrated that reflectin sequences with higher content of glutamic and aspartic acids yield materials with higher protonic current density [36].

Besides intriguing electro-optical properties, Phan and colleagues demonstrated how reflectin films can be used as effective substrate for the growth of the mammalian cells [46]. As presented in Fig. 4D, authors verified that films made of recombinant Reflectin 1A (*Doryteuthis pealeii*) facilitate cell adhesion after seeding and support their proliferation as well as differentiation [46].

2.3.2. Materials based on engineered reflectin sequences

Given the modular and repetitive architecture of the reflectins sequence, there have been several works reporting engineered reflectin sequences with variable lengths. In 2012, Qin and co-workers designed a peptide-refCBA (MW = 14 kDa), a simplified version of the full-length Reflectin 1a from *Euprymna scolopes* comprising its key conserved motifs [30]. The peptide was recombinantly produced in the soluble form, significantly facilitating its purification in comparison to the full-length proteins, which are expressed in inclusion bodies and require harsh conditions for purification [50]. Additionally, due to the high refCBA solubility, water-based peptide solutions were used for film production, employing both flow-coating and spin-coating techniques. This approach not only facilitates biomaterial synthesis, but also provides more sustainable practices. Moreover, despite lower complexity, refCBA was hierarchically organized during film production and the resultant films were stimuli-responsive and changed color upon water exposure, due to thickness variations [30].

In 2017, Dennis et al. identified a small 23 amino acid region in the sequence of R1b from *Euprymna scolopes* named 2C, that reproduces the film characteristics observed in the complete protein [47]. The 4-concatemer of this peptide (Ref(2C)₄) yielded films that retain the stimuli-responsive and light-scattering properties observed with the full-length protein [47]. As a follow-up of this study, in 2021, Xu and colleagues used the same His-tagged concatemer Ref(2C)₄, to produce two-terminal devices with 4 to 8-fold higher values of bulk proton conductivity when compared to the full-length protein. Moreover, the authors showed that using a rationally engineered reflectin polypeptide enables the production of long-range proton transport (over distances of ~1 mm) [39].

Furthermore, Umerami and colleagues generated a truncated version of Reflectin A1 from *Doryteuthis pealeii* (RfA1TV) that comprises the first repeating motif of the sequence (RM) and its preceding linker region [51]. Folding variations of RfA1TV were induced by applying mechanical force. As presented in Fig. 4E, upon continuous mechanical agitations, reflectin peptides tend to gain more order and increase the β -sheet content. These variations in folding were also linked to the diverse architectural formations from the hierarchical self-assembly of the peptide (e.g. nanoparticles, beads-on-a-noodle, fibrils) [51].

While investigating the origin of reflectin genes in cephalopods, Guan and colleagues identified an octapeptide sequence that was present not only within reflectin sequences, but also in the genome of the bacteria *Vibrio fischeri* [32]. This sequence, called protopeptide, consists of YMDMSGYQ and according to their studies was transposed from bacteria to cephalopod likely due to their symbiotic interaction [32,52]. Besides the original sequence, some variants were identified and include (Y/W/G)MD(M/F)X(G/N)X₂, where X represents S, Y, Q, W, H, or R. Authors further demonstrate that protopeptide can hierarchically self-assemble into well-dispersed nanostructures [32]. More recently, Dias et al. investigated the original protopeptide sequence (YMDMSGYQ) self-assembly and took advantage of this property to produce peptide-based spun fibers using the solution blow-spinning technique [37,53]. By varying the solvent type, authors modulate protopeptide

self-assembly, forming sub-microfibers with different morphology and variable thickness [37]. In a different study, protopeptide hydrogels were produced. Through a series of experimental and *in silico* studies authors demonstrated that protopeptide chains interact via π - π stacking and H-bond interactions mediated by tyrosine. Such interaction led to the formation of β -sheets and consequently higher order structures, such as fibrils as demonstrated in Fig. 4F [51].

On a final note, it should be highlighted that reflectins applications can be further broadened. A recent investigation led by Gorodetsky's group has engineered the optical properties of mammalian cells by introducing the gene encoding for reflectin A1 from *Doryteuthis pealeii* through transfection [40,48,49]. The combination of the genetically engineered mammalian cells and microscopy techniques revealed the effective expression of reflectin within the cells and the formation of highly polydisperse spheroidal nanoparticles (with a diameter <1000 nm) and irregularly shaped nanostructures (d >200 nm), closely resembling leucosomes size [40,48,49]. The formed reflectin-based nanostructures showed a higher refractive index (≥ 1.42) in comparison to other cellular components (typically <1.40) [48,54]. Cell exposure to chemical stimuli (100 mM NaCl) causes aggregation of reflectin-based formations giving rise to larger and more polydisperse assemblies with higher refractive index (shifting from 1.41 to 1.43 to 1.44–1.46). Consequently, this alteration influenced the transparency of cells and their light-scattering ability, as demonstrated in Fig. 4G [48,49]. This study underscores the potential of reflectin-based nanostructures in cell engineering, paving the way for novel applications in areas such as bioimaging, biosensing, and optogenetics.

3. Histidine-binding proteins and inspired materials

3.1. The biological context of histidine-binding proteins

Beaks are one of the very few hard parts of cephalopods body used for hunting and feeding [55]. The squid beak is composed by proteins (50 %), chitin (15–20 %) and other organic materials (30–35 %) and is divided in two parts: the wing (base of the beak) and the rostrum (tip). Among other biological structures, squid beak composition is most similar to the insect exoskeleton [56]. The beak mechanical properties are determined by the water content and the chemical crosslinking between chitin and two proteins: Chitin-binding protein (CBP) and Histidine-binding protein (HBP) [57,58]. The water, chitin and protein content vary gradually along the beak which influences their mechanical properties (Fig. 6A). There is a decrease of hardness and stiffness from the rostrum to the wing accompanied by a significant increase of water concentration and chitin content and a decrease in protein quantity [57,59]. CBPs and HBPs play a distinct and interconnected role in maintaining the beak structure. CBPs form hydrogen-bonds with chitin, altering its hydrophobic properties and forming a well-hydrated scaffold. This ensures high flexibility of the attachment point of the beak in the buccal mass. HBPs mechanically stabilize, infiltrate and strengthen the beak scaffold while stiffening it due to dehydration caused by HBPs ability to form coacervates. So, the wing, being the softer region of the beak, does not present HBPs [57,60]. To date, only the beak proteins of Humboldt squid (*Dosidicus gigas*) were explored even though histidine-rich proteins were found in *Doryteuthis pealeii* and *Euprymna scolopes* [61]. As CBPs are present in other organisms and they have been widely studied and reviewed [62–64], we will focus our analysis on the unique histidine-binding proteins of cephalopods and their applications in materials science.

3.2. Organization and assembly of histidine-binding proteins

Histidine-binding proteins (HBPs) are predominantly hydrophobic with a high content of glycine, alanine and histidine residues (over 50 %) and with an isoelectric point around 6. Three histidine-rich beak proteins - HBP1, HBP2 and HBP3 - have been reported so far (Fig. 5)

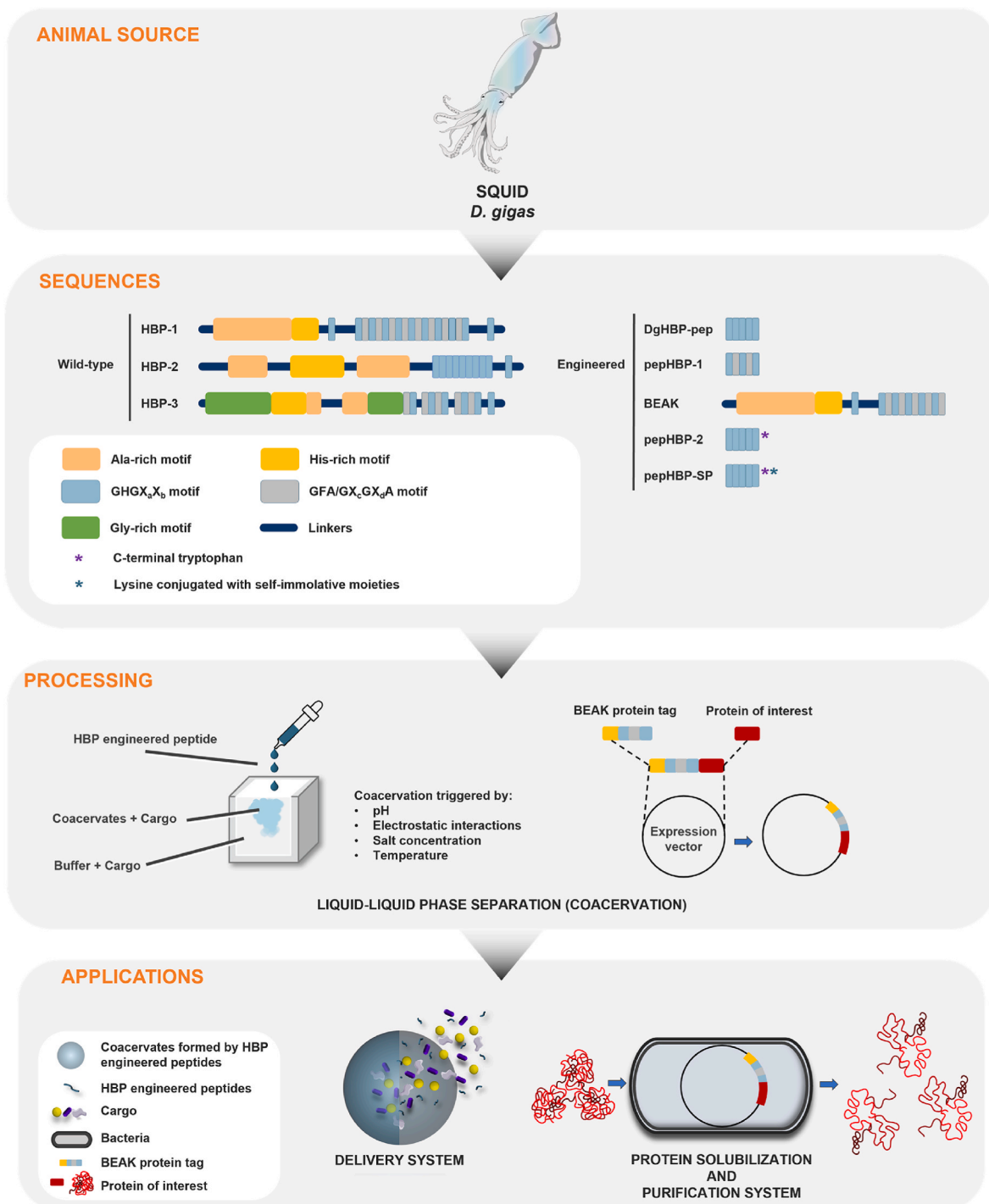


Fig. 5. Overview of histidine-binding proteins pathway from animal sources to practical applications. Histidine-binding protein 1 and 2 were engineered and investigated with a special focus on the repeating motifs found in their C-terminal due to their ability to coacervate. X represents any amino acid, but usually it is proline, valine, leucine, tyrosine or histidine. So far, the reported applications rely exclusively on engineered peptides.

[57].

The N-terminal of HBPs is non-repetitive and composed of Gly-, Ala- and His-rich regions. The length is variable since the number of Ala-rich regions and the size of His-rich domains present is not constant [57,65].

The C-terminal portion of HBPs is predominately hydrophobic, with repetitive motifs that may be interspersed by linkers. It usually consists of two typical pentapeptide sequences: GHGX_aX_b motif and GFA/GX_cGX_dA motif. In the GHGX_aX_b motif, histidine residues are flanked by Gly residues where X_a is usually a hydrophobic residue, such as proline, valine or leucine; while, X_b is usually a tyrosine, but it can also be a

histidine. This motif is similar to the hydrophobic repeats rich in glycine and valine responsible for elastin self-coacervation [57,66]. The most common variations of the pentapeptides are GHGPY and GHGLY (Fig. 5, in light blue) [57]. The other typical motif is the GFA/GX_cGX_dA, where X_c is typically proline or alanine; while, X_d is either phenylalanine or tyrosine. The presence of this motif, namely the modular peptide GAGFA or GFA is optional in HBPs sequences. Its absence in HBP-2 suggests that its role is not related with self-coacervation but with β -sheet stabilization (Fig. 5, in orange) [65,67].

HBPs are IDPs that can partake in LLPS (Fig. 6A) [60,68].

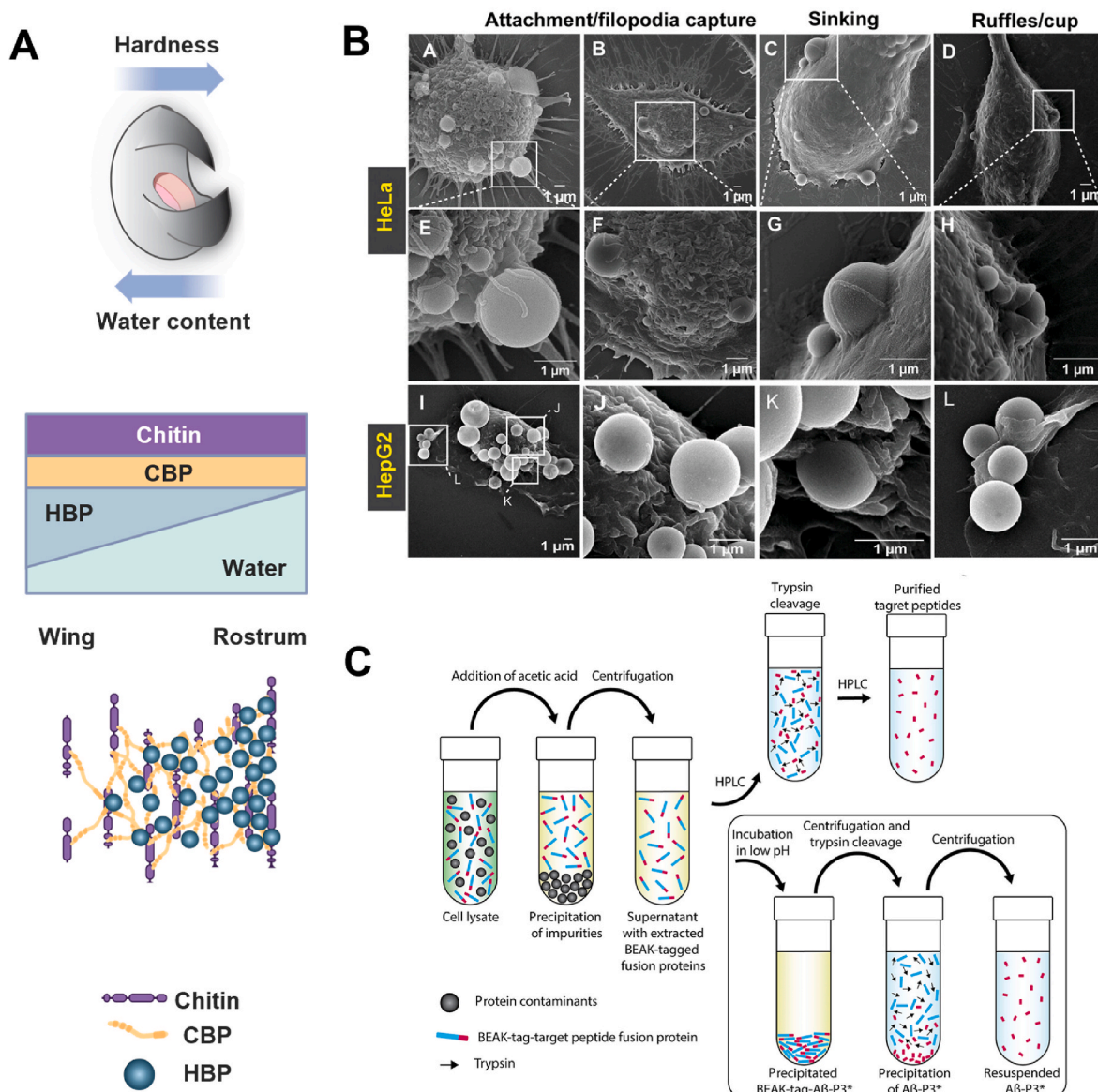


Fig. 6. Cephalopod beak, coacervation process of HBP and a non-cargo release application. (A) The beak's mechanical properties are highly influenced by the water content. Cross-linking and coacervation contribute to the formation of a cohesive network essential for the beak's mechanical properties. Created in BioRender. Roque, C. (2025) <https://BioRender.com/e19b085> (B) SEM images showing the initial stages of pepHBP-2 and HBpep-SR coacervates uptake in HeLa and HepG2 cells, respectively. Reproduced under terms of the CC-BY license [82]. Copyright 2025, A. Shebanova et al., published by John Wiley and Sons. (C) Representation of the protein solubilization system showing the purification process of BEAK-tagged amyloidogenic peptides. Reproduced with permission [75]. Copyright 2025, John Wiley and Sons.

Coacervation of HPBs starts when there is a change in pH - the deprotonation of histidine side chains, namely through the GHGX_aX_b region [60,65], alters the protein net charge and triggers hydrophobic intermolecular interactions controlled by Tyr-Tyr interactions (aromatic stacking of side chains) leading to coacervate condensation [60]. It has been found that the pentapeptide GHGLY is particularly important to LLPS and should be present in 4 consecutive repeats. Alternatively, there should be at least two repeats of the pentapeptide GHGLY, separated by a spacer with enough conformational flexibility. This spacer should be composed of at least three copies of GHGLH/GAGFA or a combination of the peptides GAGFA/GFA and GHGHL [60,65].

Considering the distinct architecture of HBP-1 and HBP-2 conserved domains, Cai designed two peptides: (i) pepHBP-1 with HBP-1 residues G¹¹² to Y¹³⁵ (GHGLY GAGFA GHGLH GFA GHGLY), and (ii) pepHBP-2, composed by a consensus sequence of 26 amino acids - (GHGXY)₅W, where X can be either valine, proline or leucine - derived from the HBP-2

protein.

pepHBP-1, just like the full-length protein, showed a higher G' (10^1 Pa) than pep-HBP-2 (0.1 Pa). These results, adjoined with the CD spectra, point to the importance of GAGFA and GFA motifs to the formation of β -sheet domains and the enhancement of the physical cross-linking density in the coacervates [65]. On the other hand, pepHBP-2 presented liquid-like behavior since G' was smaller than G'' . This peptide presented self-coacervation behavior under pH 8 and 0.5 M ionic strength (conditions similar to seawater pH and salinity), further proving the role of the GHGXY repeats to drive beak maturation due to coacervation [57].

3.3. Soft materials based on histidine-binding peptides and proteins

Peptide-derived from HBPs have been engineered and explored in applications related to their potential to spontaneously self-condensate

in aqueous environments and to form coacervates under defined conditions. Table 3 provides a comparative analysis of key features of wild-type HBP sequences and engineered peptides, as well as reported applications (also in Fig. 6).

A first study reported pepHBP-2 peptide coacervates in aqueous buffer conditions, which were used to encapsulate glucose oxidase and insulin with near 100 % efficiency. In an environment with high concentration of glucose, the monosaccharide diffuses into the coacervates. Glucose is then converted to gluconic acid by the glucose oxidase creating an acidic environment that triggers the dissociation of the coacervates and the consequent release of insulin. The amount of insulin released is proportional to the glucose concentration in the blood stream and can be done at least 3 times, with only a portion of insulin being released at each time. This system presents low toxicity and preserves the integrity of the cargo but still has some leakage when there is no glucose present. The authors suggested that this can be minimized by either mutating some of the amino acids in the peptide or by adjusting the number of tandem pentapeptides [69].

In a different study, a pepHBP-2 crosslinked coacervate was explored as a vehicle for liver cancer therapy via thermo-chemotherapy. The chemotherapeutic drug Doxorubicin and magnetic nanoparticles were enclosed within the microdroplets formed by the coacervates. These cyto-compatible coacervates are guided to the target cells via an external

magnetic field. When it is inside the cancerous cells, the drug is released by applying an external alternating magnetic field, that will be followed by a rise in temperature that stimulates the disintegration of the coacervates leading to a controlled release of the carrier molecules leading to HepG2 liver cancer cell death. It is worth to notice that there was some cargo release at physiological temperature, but the majority was released between 42 °C and 45 °C. Due to the nanoparticles, this system can be used for both therapy and diagnostics since their magnetic properties provide means for imaging to monitor the treatment having real-time assessment of the treatment efficiency. The combination thermo-chemotherapy treatment was more successful than either treatment alone [70].

The sequence of pepHBP-2 was further altered by adding a lysine single point mutation in position 16 (pepHBP-K) which switched the phase separation pH from 7.5 to 9. Afterwards, a disulfide containing moiety was added to the new lysine of pepHBP-K to neutralize the positive charge, increase the total hydrophobicity of the peptide and triggering redox responsiveness. Finally, an acetyl and a phenyl group were added to the extremity of the self-immolative moiety so that the phase separation occurred at a pH lower than 6.5. The modified pepHBP-K (pepHBP-SR) formed pH and redox-sensitive coacervates used for cargo release across the cytoplasm. Once inside the cells, the cargo is released via redox reactions, mainly due to glutathione-

Table 3

Key features and applications of wild-type and engineered Histidine-binding protein and peptide sequences.

Protein name/Uniprot ID	Species	MW (kDa)	pI	Key features	Applications	Ref.
Wild-type proteins						
HBP-1/A0A0G2UMW8	<i>D. gigas</i>	15.2	6.03	Expressed in the insoluble fraction. High solubility at low pH. Self-coacervate in pH near physiological but pH window can be broadened increasing ionic strength. Coacervates present shear-thinning behavior. Rheology shows gel-like behavior. Several peptides were engineered from this sequence to study the pentapeptide GHGXY ability to phase separate.	Not described	[57,60,65]
HBP-2/A0A0G2UHG9	<i>D. gigas</i>	18.2	6.15	Protein expressed in the insoluble fraction. High solubility at low pH. Self-coacervate pH near physiological but pH window can be broadened increasing ionic strength. Coacervates can have a size of ~1 µm. Coacervates do not appear to have shear-thinning. Rheology shows gel-like behavior	Not described	[57,65,78]
HBP-3/A0A0G2UJ03	<i>D. gigas</i>	15.1	6.5	Long Gly-rich repeats	Not described	[57]
Engineered peptides						
pepHBP (also referred as DgHBP-pep)	<i>D. gigas</i>	^{a)} 2.6	^{a)} 7.15	Mostly hydrophobic. Self-coacervation. In conditions similar to sea water, it is between precipitation and coacervation.	Not described	[57]
pepHBP-1 (also referred as GY23).	<i>D. gigas</i>	^{a)} 2.2	^{a)} 7.10	Residues G113–Y135 of HBP-1. Rheology shows gel-like behavior. Several variants were made to study the impact of single mutations in coacervates viscoelastic properties.	Not described	[65,79]
BEAK	<i>D. gigas</i>	^{a)} 5.46	^{a)} 10.6	N-terminal and part of C-terminal of HBP-1	Efficient tag that facilitates proper protein folding and function and simplifies purification in soluble fraction of difficult to express proteins	[75]
pepHBP-2 (also referred to as HBpep, DgHBP-2 peptide and GW26)	<i>D. gigas</i>	2.8	7.9	5 repeats of the GHGXY and a single C-terminus Trp residue. Rheology shows liquid-like behavior. High loading capacity. Without cargo, coacervates can have a size of ~1 µm. Non-cytotoxic. Good encapsulation efficiency. Several variants were made	Cargo release: insulin; doxorubicin and nanomagnetic particles; aggregation-induced emission (AIE)-fluorogen;	[65,69,70,74,76]
HBpep-SR (also referred to as HBpep-SP)	<i>D. gigas</i>	2.9	8.37	Lysine conjugated with self-immolative moieties added to increase coacervation pH. High loading capacity. Very efficient delivery system when compared with other commercially available. Protects cargo from degradation. Redox-driven disassembly. Non cytotoxic. Several variants were made.	Cargo release: enhanced green fluorescence protein (EGFP); Alexa Fluor 488 (AF)-labelled lysozyme; Bovine serum albumin (BSA); R-phycoerythrin (larger red fluorescence protein (R-PE)); Saporin; β-galactosidase, mitochondria-derived activator (Smac, AVPIAQQ); proapoptotic domain (PAD, KLAKLAK KLAKLAK); anticancer peptides (dPMI-δ, MP-189 and MP-950); CRISPR/Cas-9 machinery (pDNA, mRNA/sgRNA and ribonucleoprotein)	[71–73,76,77,80]

^{a)} Indicates that the MW and pI were not reported in the literature and were calculated using the Prot/Param tool on the EXPASY server.

mediated mechanisms. They have the capacity to efficiently recruit, carry and release with high efficiency small peptides (726 Da), larger proteins (430 kDa) and mRNA. It was proven that the mRNA is protected from RNase activity, opening the possibility of this technology to be used for mRNA-based therapies and vaccines. It is to note that this system can also be used as a mean to increase transfection and subsequent gene editing efficiency due to its ability to encapsulate and transport the components of the CRISPR/Cas9 system, particularly the Cas9 protein in its native form, something than the usual vehicles are not as effective [71–73].

The potential to rationally engineer the sequence of pepHBP-2 was further studied. Variants of pepHBP-2 were designed bearing the OmpT recognition site (2 arginine residues) positioned between the GHGXY pentapeptides. Peptide coacervates were formed in the presence of a fluorogen which remained encapsulated. The signal emission occurs when fluorogen molecules aggregate due to proximity at high concentrations, and thus it detects LLPS via aggregation induced emission. As OmpT is an *E. coli* outer membrane protease, peptide coacervates were cleaved in the presence of the bacteria, and thus the coacervates were disassembled and fluorescence altered. This method enabled the detection of *E. coli* by naked eye in the presence of UVA light [74].

Another creative application for HBP-derived peptides and their coacervates was reported considering that the N-terminal domain of HBPs does not partake in LLPS and might facilitate the expression of the aggregation-prone C-terminal. Gabryelczyk et al. designed a tag (BEAK-tag) derived from HBP-1 peptide comprised of the N-terminal and part of the C-terminal that has a role in coacervate formation. With this tag, usually difficult to obtain amyloidogenic and hydrophobic peptides were successfully recombinantly expressed by avoiding early aggregation of the protein during overexpression. The expression is then done without undesired chemical modifications and in the soluble fraction resulting in an inexpensive, fast and high yield procedure. Furthermore, the formed membraneless organelles further facilitated purification by a chromatography-free method while preventing premature aggregation (Fig. 6C) [75].

4. Sucker ring teeth proteins and inspired materials

4.1. The biological context of suckerins

Sucker ring teeth (SRT) are present in the suction cups lining the tentacles of cephalopods, in particular squids and cuttlefish. Tentacles are used to strongly hold onto prey through contraction of the sucker muscles, causing an inward motion of the triangular teeth to pierce through skin and scales [81,82]. Due to its predatory function, SRT are exposed to elevated shearing and compressive forces, demanding a combined degree of mechanical robustness and flexibility [81]. SRT is quite unique as it only contains proteins in its composition – denominated Suckerins. SRT exhibits exceptional mechanical properties, with an elastic modulus, ranging from the tooth core to the periphery between 4.5 and 7.5 GPa in the dried state and 1.75–2.75 GPa when hydrated, respectively [82], to an elevated thermal resistance [83]. These values are comparable to spider silk fibers, with elastic modulus ranging from 0.012 to 13.8 GPa (variation depends on the spider species) [84–86].

4.2. Suckerins organization and assembly

Suckerins contain an elevated content of glycine, tyrosine and histidine residues. Other prominent amino acids are leucine, alanine, valine, threonine, serine and proline [82,83]. These amino acids arrange themselves into modules M1 and M2.

Module 1 [M1] is rich in Ala, Val, Thr, Ser, and His residues and has a length of 11 residues [81,83]. It forms a crystalline domain that drives the formation of β -sheets, providing mechanical strength to the SRT, reminiscent to the crystalline domains found in spider dragline silk [87].

[M1] modules are composed by hydrophobic polypeptide sequences A1: AATAVS, A2: AAASV, A3: AATVS, and A4: ATTAVS, combined with the most abundant hydrophilic H1: HTTHHA (Fig. 7).

Module 2 [M2] is rich in Gly, Leu, and Tyr, contains between 20 and 30 residues [81,83] and forms amorphous domains. These sequences organize in flexible chains that provide plasticity and elasticity, also denoting similarity to amorphous domains in spider dragline silk [87]. Interestingly, it has been shown that a fraction of [M2] modules may also partake in β -sheet formation at elevated concentrations. In more detail, this mechanism occurs due to a conformation transition from helices to β -sheets stabilized by intrachain hydrophobic interactions, through the C-terminal Val residue and π - π stacking through Tyr residues [83,88,89]. [M2] modules contain a combination of G1: GYG, G2: GGY, G3: GGLY, and G4: GLGGY polypeptides [83,88,90].

Proline, which is known to be a β -sheet disruptor [91], often flanks [M1] modules, limiting the size of the crystalline domains and separating them from the amorphous domains [88], in such a way that the motif P[M1]P[M2] is commonly found in tandem repeats in several suckerin sequences [83].

Structural studies on suckerin derived peptides proposed the organization of the crystalline domains into stacks of five β -sheets [83] in parallel or anti-parallel orientation [92] stabilized by H-bonds and π - π stacking interactions, mainly by the histidine residues [83,88,92]. The formation of β -sheets is driven by the hydrophobic portion of the [M1] modules, while the hydrophilic His-rich fraction provides solubility in mild acidic conditions and stability to the structure [92]. Representative A1H1 peptide, AATAVSHTTHHA, revealed the organization of β -sheets and the pH-dependence of their secondary structure [92,93], while the peptide GV8, GLYGGYGV, showed β -sheet formation in the amorphous region, as previously noted [89].

Suckerins assembly is formed by nanoconfined and randomly oriented stacks of β -sheets that stabilize an amorphous domain [83,88], providing SRT with a flexible yet robust foundation, ideal to resist the shear and compressive stresses usual to prey capture.

4.3. Materials from wild-type suckerin sequences

Since their discovery, suckerin proteins have been extensively explored to produce a range of materials for distinct applications. Wild type sequences are not exclusive to this research, engineered sequences have also been designed and produced, as well as relevant peptide sequences from *D. gigas* suckerin-19 (Table 4). All forms of suckerin proteins exhibit interesting properties and applications which will be explored in the discussion below. Fig. 7 presents an overview of the suckerin pathway from its natural source to functional materials, while Fig. 8 illustrates examples of practical applications and the processing of suckerin-based materials.

Dosidicus gigas suckerin-19 has been the most characterized and explored to date. This protein stands as a suckerin family reference – it is the most abundant suckerin in *D. gigas*, it is rich in the repeat motif P [M1]P[M2] and presents a medium-range molecular weight (39 KDa) compared to other suckerin sequences [81,84].

The mechanical properties of recombinant suckerin-19 derived materials are highly tuneable [90,94]. Suckerin-19 has been processed into films, exhibiting ~ 7.5 GPa moduli in the dried state, similar to native SRT, but decreasing to 5–8 MPa in the wetted state, meeting the threshold of hydrated spider dragline silk (10 MPa). Ruthenium-based photo crosslinking of the suckerin films, through the tyrosine residues abundant in the [M2] amorphous domains, yielded an elastic modulus of 6–7 GPa in the hydrated state, very close to the moduli in the dried state (8–9 GPa). These represent the highest moduli achieved in hydrated protein-based materials, and even surpasses many polymers, in terms of modulus and hardness.

Interestingly, the elastic modulus of crosslinked suckerin was demonstrated to be inversely correlated with the crosslinking density [90]. A high crosslinking of the tyrosine residues limits chain backbone

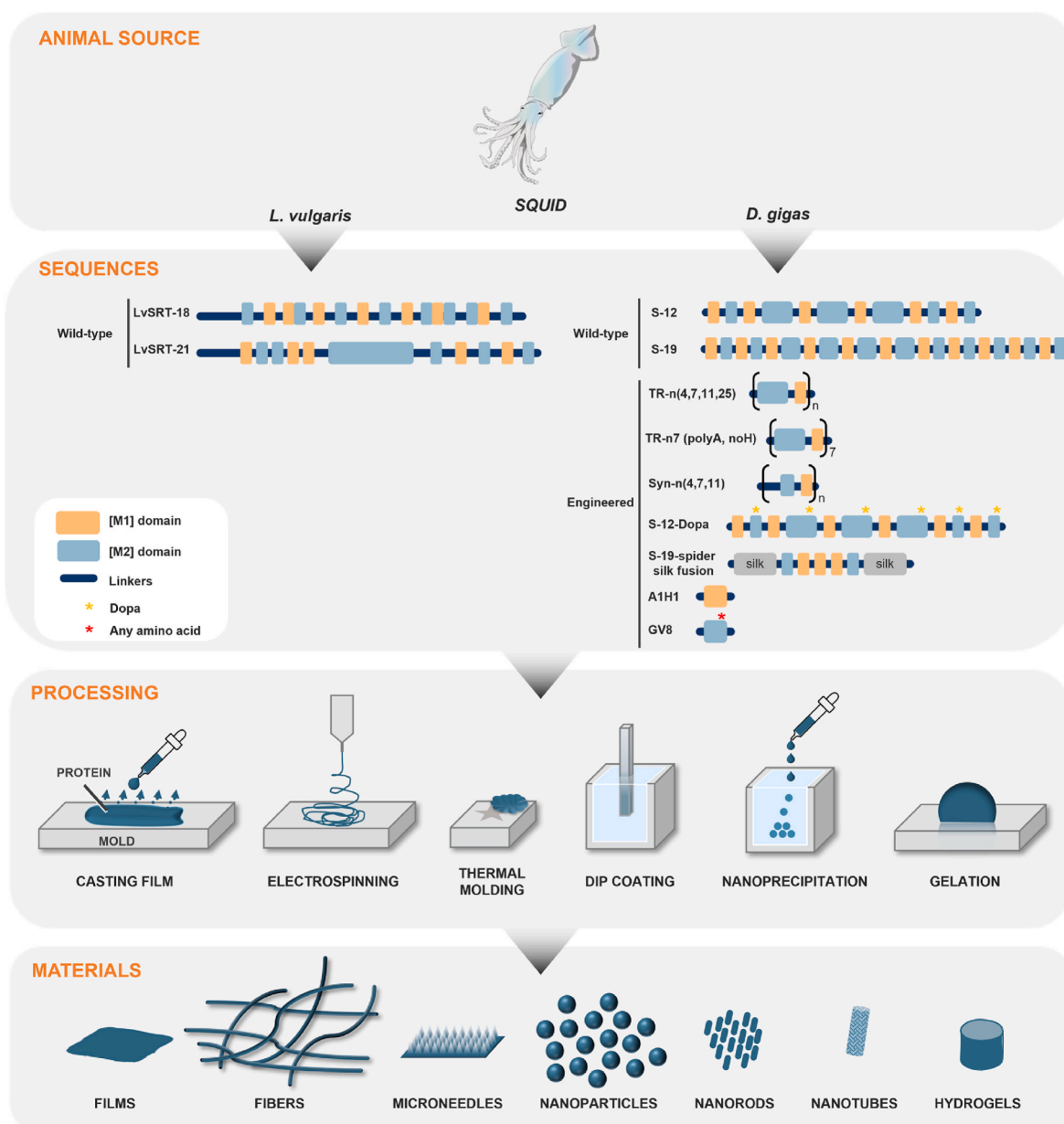


Fig. 7. Overview of suckerins pathway from animal to functional materials. Suckerins from *L. vulgaris* and *D. gigas* squids are being extensively studied and engineered for the development of bio-based functional materials through a variety of techniques.

flexibility, therefore inhibiting β -sheet formation. Exploiting this property, the elastic moduli of suckerin has been tuned down to the range of 100 MPa, yielding soft materials, like hydrogels (Fig. 8B).

An alternative mode of enzymatic crosslinking, using horseradish peroxidase (HRP), has also been implemented on recombinant suckerin-12, a smaller isoform of SRT derived from *D. gigas* [95]. The enzymatic crosslinking of suckerin-12, which is based upon the same principle of di-Tyr covalent bonding between the [M2] amorphous domains, allowed the preparation of mechanically stable hydrogels, which was not possible to achieve using the afore-mentioned Ruthenium-based photo crosslinking method.

Biocompatibility and cell viability has been demonstrated in recombinant suckerin-19, by growing human stem cells on suckerin-19 films [94]. Immortalized human keratinocytes (HaCaT) and primary human dermal fibroblasts (HDF) cells were also attached on bioinspired octapeptide, GV8, hydrogels, and a healthy cell morphology after attachment was demonstrated (Fig. 8B) [96]. Additionally, suckerins have an inherent anti-bacterial activity, as a result of being positively

charged at near neutral pH, due to presenting typically high isoelectric points [97], with the correlation between positively charged bio-materials and antibacterial capacity already being an well-known feature [97].

Due to its biocompatibility, suckerin-19 has been exploited as a drug carrier agent, in the form of precipitated di-Tyr crosslinked nanoparticles, with a uniform size distribution [98]. Amphiphilic by nature, precipitated suckerin-19 nanoparticles contained a hydrophobic β -sheet interior in aqueous solution, into which therapeutic drugs could be loaded. With a His-rich interior, the rate and extent of drug release could easily be modulated by pH, repelling the drug molecules by protonation of the His residues. The cytotoxicity and antitumoral effect of drug-loaded suckerin nanoparticles has thus been proven both *in vitro* and *in vivo* systems, with suckerin facilitating intracellular drug delivery and ensuring continued high drug concentration in the tumour site, by controlled drug release. These particles were also tested as gene carriers of plasmid DNA [98]. Similar to drug encapsulation, DNA was condensed and stabilized by non-electrostatic interactions with the

Table 4

Comparative analysis of key features and potential applications of wild-type, engineered and peptides derived from suckerin proteins.

Protein name/ Uniprot ID	Species	MW (kDa)	pI	Key features	Applications	Ref.
Wild-type proteins						
LvSRT-18/ ^{a)} NA	<i>L. vulgaris</i>	18.0	8.09	Self-healing capability; Reversible glass-to-rubber transition	Fuel cells, controlled release tech, self-healing patches	[100,112,114]
LvSRT-21/ ^{a)} NA	<i>L. vulgaris</i>	21.0	8.07		Self-healing textiles	[100,113]
Suckerin-12/ A0A075LXT7	<i>D. gigas</i>	24.3	8.04	Modular repeats; Antibacterial activity; Biocompatibility	Biomedical, biosubstrates for forming gold nanoparticles	[83,95,99,108,115]
Suckerin-19/U5NYJ1	<i>D. gigas</i>	39.0	8.33	Most abundant in <i>D. gigas</i> ; Modular repeats; Medium-range molecular weight; Antibacterial activity; Biocompatibility	Biomedical, photonics, sensing devices, biosubstrates for forming gold nanoparticles	[83,84,90,94,98,99]
Engineered proteins and peptides						
TR-n4	–	15.0	7.07	Conductive properties; Increased toughness with repeats	Conducting materials	[102–104]
TR-n7	–	25.0	7.24			[102–104]
TR-n11	–	42.0	7.37			[102–104]
TR-n25	–	86.0	7.56			[102–104]
Tr-n7 (polyA, noH)	–	25.0	5.27	Altered conductive properties in the absence of histidine residues		[102–104]
Syn-n4	–	15.7	7.09	Increased toughness and extensibility with repeats; constant elastic modulus and yield strength	Template for electrode printing, thermal actuators	[105–107]
Syn-n7	–	25.8	7.25			[105–107]
Syn-n11	–	42.7	7.40			[105–107]
Suckerin-12-Dopa	<i>D. gigas</i>	24.8	–	Enhanced wet-resistant adhesive properties	Biomedical	[108]
Suckerin19-Spider Silk Fusion Protein	<i>E. australis</i> + <i>D. gigas</i> + <i>A. ventricoccus</i>	33.1	–	Precisely defined nanocapsules hydrogels	Drug release	[109,116]
A1H1	<i>D. gigas</i>	12.0	7.06	Self-assembles into β -sheet amyloid like-fibrils	Biomembranes, biosensors, energy conversion devices	[89,110]
GV8 (GX8)	<i>D. gigas</i>	7.84	5.52	Undergoes 3 ₁₀ -helix to β -sheet transition, with increase of concentration in water; Hydrogels	Biomedical	[89,111]

^{a)} NA – Not available.

hydrophobic β -sheets within the nanoparticles. Gene transfection was shown effective, and despite being lower than for polyethylenimine (PEI) nanoparticles, suckerin-19 presented negligible cytotoxicity, thus allowing higher dosage of therapeutic DNA.

In another work, drug-bearing microneedle arrays of suckerins extracted from SRT were fabricated by soft lithography in a PDMS mold [97]. The Young Modulus of the formulated microneedles could easily be tuned by exposure to solutions of different pH, and in turn, modulate the release kinetics of drugs subcutaneously *in vitro* models, which has not been reported in other bio-based microneedle materials. A simple application of the suckerin microneedles with a urea solution (present in dermal creams up to 4M), could release ~2 % of the total encapsulated drug, which is comparable to commercially available alternatives. The intrinsic antibacterial activity of suckerins, as mentioned above, also added to the increased safety of employing these materials as microneedle devices, reducing the risk of infection, as demonstrated by the measurement of colony forming units, in comparison to standard microneedle materials, presenting a reduction in cell density of four orders of magnitude.

The abundant Tyr residues found in suckerin-19 and suckerin-12 have been used as templates for the deposition of gold nanoparticles, by acting as reducing agents of HAuCl₄ salts into Au [99]. Gold nanoparticles can be used for biomedical applications (e.g. as drug carriers), where inhibiting aggregation of particles is crucial for maintaining the desired properties. The elevated Tyr content of suckerins (up to ~15 %) allowed the spatially controlled deposition of Au nanoparticles, compared to other silk alternatives [99].

Suckerins from *Dosidicus gigas* have been the most extensively studied proteins for materials' production and applications, but a few suckerins from *Loligo vulgaris* and *Sepiotheutis lessoniana* have also been exploited and processed into interesting biomaterials.

Suckerins in their native form typically present reversible thermoplastic properties. Recombinant expressed suckerin-19 lacks this feature, only allowing processing in solution phase. Recombinant

suckerin from *L. vulgaris* (LvSRT-18) preserved its thermoplasticity, which was attributed to its smaller size, compared to suckerin-19, due to the increased amount of hydrogen bonding in the smaller proteins [100].

The lack of covalent interactions confers suckerins an exceptional thermal processability, on par with commercial synthetic polymers. Heating the protein in water is enough to obtain a fully processable material. Because the β -sheet crystal lattice remains intact up to a degradation temperature of 220 °C, the mechanical properties of suckerins are fully reversible, allowing it to be reshaped and reused multiple times, in a wide thermal spectrum [101]. These features make suckerins a sustainable alternative to synthetic thermoplastics derived from fossil fuels, an acknowledged environmental concern.

4.4. Materials from engineered suckerin sequences

Several suckerin variant sequences have been designed [102–107]. Tandem repeat (n = 4, 7, 11, and 25) polypeptide sequences were designed, based on the amorphous domain YGYGGLYGGYGLGYG, and the crystalline domain PAAASVSTVHHP [102]. The increase in tandem repeats correlated linearly with the tensile modulus and ultimate toughness [103], highlighting the relation between tandem repetition and the rheological properties of suckerins. These sequences could be explored to fabricate materials that require these properties, such as biosensing or tissue engineering.

A recombinant form of *D. gigas* suckerin-12 has also been expressed using residue-specific incorporation of 3,4-L-dihydroxyphenylalanine (Dopa) in replacement of Tyr residues in the amorphous domain. This synthetic biology strategy allowed to enhance wet-adhesion kinetics to produce wet-resistant adhesive films with suckerins. The results were very promising, as suckerin glues exceeded the adhesive properties of mussel proteins (the gold standard for marine adhesive properties) [108].

Another study has combined suckerins with spidroin domains from

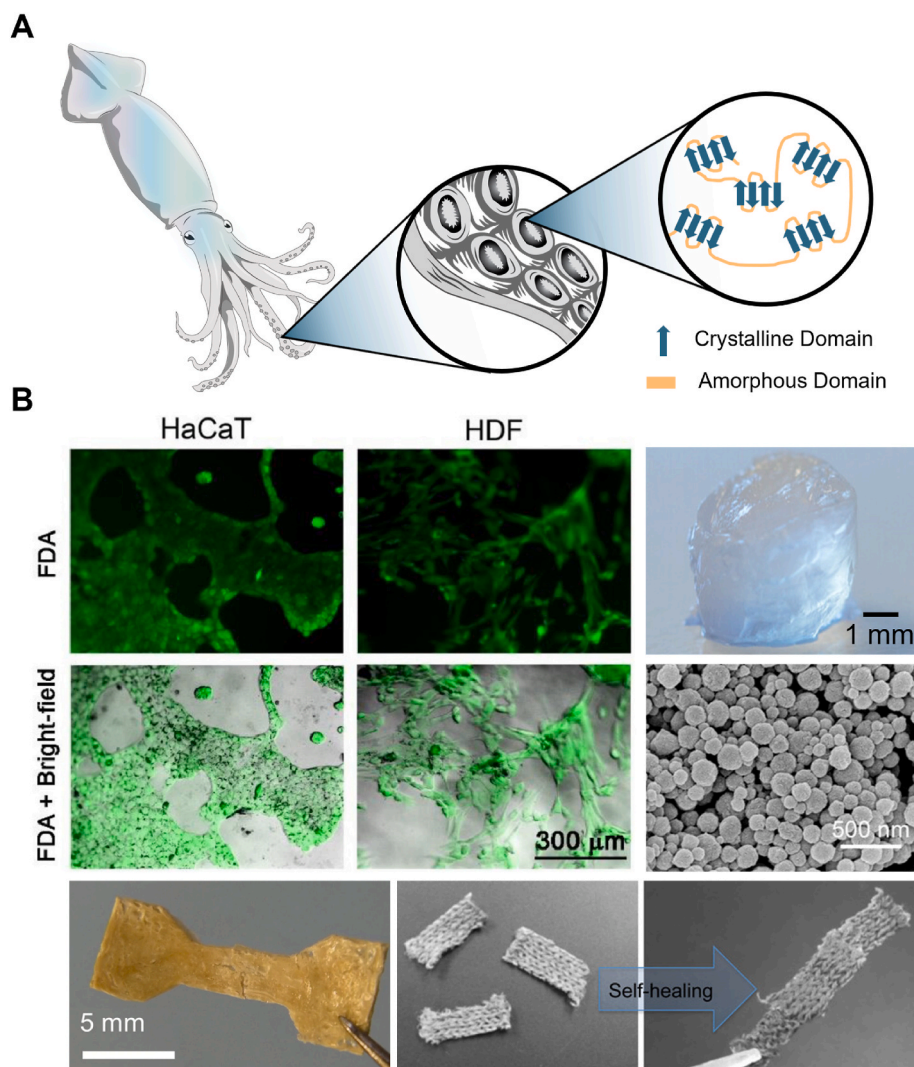


Fig. 8. Suckerins biological context, structure and applications (A) SRT proteins, located in the suction cup, provide toughness and elasticity due to the formation of β -sheets. (B) Examples of the practical applications and processing of suckerin-based materials. Top left: Illustration of immortalized human keratinocytes (HaCaT) and primary human dermal fibroblasts (HDF) cells on bioinspired octapeptide, GV8, hydrogels. Images of live cells stained with fluorescein diacetate (FDA), top row, and overlay of FDA and bright-field images, bottom row, demonstrate healthy cell morphology after attachment. Reproduced with permission [96]. Copyright 2025, Elsevier. Top right: Photograph of a 10 mM G18 peptide hydrogel prepared in a syringe barrel mold. Reproduced with permission [111]. Copyright 2025, American Chemical Society. Middle right: SEM image of recombinant S-19 nanoparticles with controlled particle sizes of 100–200 nm. Reproduced with permission [98]. Copyright 2025, American Chemical Society. Bottom left: Recombinant SRT-18 was expressed and molded into a dog bone shaped beam showing the thermoplastic properties. Reproduced under terms of the CC-BY license [112]. Copyright 2025, Sariola, V. et al., published by Springer Nature Limited. Bottom right: Example of a self-healing textile. An SRT-coated cotton fiber was produced and cut into three pieces. Then, it was repaired by applying pressure and warm water. Reproduced with permission [113]. Copyright 2025, American Chemical Society.

spider silk, to produce suckerin-silk fusion proteins, for the construction of precisely defined nanocapsules by controlled nanoprecipitation [109]. A suckerin construct containing hydrophobic modular β -sheet forming peptides PAATAVSHTHHA and amorphous peptides GLGGYG-GLYGGY, derived from suckerin-19, was flanked by water soluble N-terminal and C-terminal domains from spider silk, of *E. australis* and *A. ventricosus*, respectively, providing solubility at neutral pH. The nanoprecipitation of the fusion protein yielded nanocapsules of precise diameters, while performing nanoprecipitation of the suckerin sequence alone resulted in an ill-defined mixture of protein capsules and aggregates. These materials serve as good platforms for the delivery of therapeutics through biocompatible protein-based nanocapsules and other encapsulation applications.

Single polypeptide sequences derived from suckerin-19 have also been exploited. These sequences allow simpler peptide chemical synthesis and purification protocols [81,89,110] and have found

applications, such as: i) Ala- and His-rich peptides produced amyloidogenic materials [110]; ii) Gly-rich peptides self-assembled into hydrogels in aqueous media, and displayed easily tuneable concentration-dependent properties [89]; as well iii) finding possible applications as soft tissue adhesives [89]; or iv) drug encapsulation [89].

5. Conclusion and future perspectives

Every day we dive deeper into the intricate mechanisms of nature. These discoveries drive innovation, inspiring more efficient, sustainable, and transformative solutions. Cephalopods are part of this phenomenon as their unique skin, beak, and ring teeth compositions have sparked scientific breakthroughs worldwide, leading to novel materials and technologies. At the root of this potential are the unique properties that reflectins, histidine-binding proteins, and suckerins possess, which can be explored to develop novel biomaterials.

Since their discovery, reflectins have been studied intensively to understand their *in vivo* mechanism and how they allow light manipulation in cephalopods cells. Scientists have also tried to use these proteins to mimic the light manipulation effect namely through thin films. These materials showed interesting properties, such as proton conductivity, stimuli responsiveness, and a high refractive index. These allow applications ranging from ionic conductors to responsive coatings and cellular optical engineering.

Histidine-binding proteins have been studied due to their ability to partake in liquid-liquid phase separation and to form coacervates. These coacervates can be used for high-efficiency encapsulation and subsequent controlled release of compounds. HBPs and engineered peptides derived from HBPs, which can form coacervates, have been used as very efficient delivery systems that protect cargo from degradation and redox-driven disassembly. This technology rivals existing commercially available vehicles, and using these peptides allows for the introduction of several point modifications that can be made to meet specific requirements. This makes HBP coacervates a very versatile and promising new approach for preventing and treating diverse diseases ranging from diabetes to cancer.

Finally, suckerins have been studied due to the elevated degree of mechanical robustness and flexibility they provide to the sucker ring teeth of squids and cuttlefish. They self-assemble into robust supramolecular structures that form a semicrystalline polymer reinforced by nano-confined β -sheets, resulting in a network with mechanical properties rivaling those of the strongest engineered polymers. Suckerins have demonstrated several interesting properties, such as glass-to-rubber transition, thermoplasticity, thermal conductivity, and modulated toughness. These lead to potential applications in various areas, from biomedical applications to conducting materials, sensing devices, and bioplastics.

Thanks to the efforts of several research groups over the past decades, the field of protein-based materials has matured to a point in which the design of function can be finely tuned by the encoded genetic sequence, with potential to replace petroleum-based materials. Still, there are several challenges to be addressed in the coming years. One aspect refers to the production by recombinant expression in host cells, which requires carbon sources that may compete with food resources. Thus, low-cost carbon sources as CO₂ from atmosphere or industrial emissions are promising avenues to increase scalability and reduce environmental impact of the manufacturing stage. Other challenges are associated with the implementation of scalable downstream processes that help reduce the final cost of the product with the required purity, as well as water consumption and waste generated. Finally, the processing of proteins into a variety of materials should avoid the use of toxic solvents that perpetuate eternal chemicals in the environmental loop. This can be achieved by fine tuning protein sequence to increase solubility in environmentally friendly solvents. Thus, carbon neutrality deserves special attention for the implementation of protein-based materials, as one must take into account the full loop from production to biodegradation after use.

CRediT authorship contribution statement

Iana Lychko: Writing – review & editing, Writing – original draft, Methodology, Conceptualization. **Inês Padrão:** Writing – review & editing, Writing – original draft, Methodology. **Afonso Vicente Eva:** Writing – review & editing, Writing – original draft. **Catarina Alexandra Oliveira Domingos:** Writing – review & editing, Writing – original draft, Methodology. **Henrique Miguel Aljustrel da Costa:** Writing – original draft, Methodology. **Ana Margarida Gonçalves Carvalho Dias:** Writing – review & editing. **Ana Cecília Afonso Roque:** Writing – review & editing, Writing – original draft, Supervision, Resources, Project administration, Funding acquisition, Conceptualization.

Declaration of competing interest

The authors declare that they have no known competing financial interests or personal relationships that could have appeared to influence the work reported in this paper.

Acknowledgements

The authors acknowledge funding from the European Research Council under the EU Horizon 2020 research and innovation programme (SCENT-ERC-2014-STG-639123, 101069405-ENSURE-ERC-2022-POC1 and 101158248-UNMASK-ERC-2023-POC), the European Union's Horizon 2020 programme under grant agreement no. 899732 (PURE project), and from FCT – Fundação para a Ciência e Tecnologia, I.P., through the projects PTDC/BII-BIO/28878/2017, PTDC/CTM-CTM/3389/2021, Research Unit on Applied Molecular Biosciences – UCIBIO (UIDP/04378/2020 and UIDB/04378/2020), Associate Laboratory Institute for Health and Bioeconomy – i4HB (LA/P/0140/2020), and the research fellowships SFRH/BD/147388/2019 for IL, UI/BD/151154/2021 for IP, 2022.11589.BD for CD and SFRH/BD/149131/2019 for HMC.

I.L. and I.P. contributed equally to this work.

Data availability

Data will be made available on request.

References

- [1] A. Miserez, J. Yu, P. Mohammadi, Protein-based biological materials: molecular design and artificial production, *Chem. Rev.* 123 (2023) 2049–2111, <https://doi.org/10.1021/acs.chemrev.2c00621>.
- [2] L.M. Mäthger, N. Shashar, R.T. Hanlon, Do cephalopods communicate using polarized light reflections from their skin? *J. Exp. Biol.* 212 (2009) 2133–2140, <https://doi.org/10.1242/jeb.020800>.
- [3] S.H. Hiew, A. Miserez, Squid sucker ring teeth: multiscale structure-property relationships, sequencing, and protein engineering of a thermoplastic biopolymer, *ACS Biomater. Sci. Eng.* 3 (2017) 680–693, <https://doi.org/10.1021/acsbomaterials.6b00284>.
- [4] R. Hanlon, Cephalopod dynamic camouflage, *Curr. Biol.* 17 (2007) 400–404, <https://doi.org/10.1016/j.cub.2007.03.034>.
- [5] L.M. Mäthger, R.T. Hanlon, Malleable skin coloration in cephalopods: selective reflectance, transmission and absorbance of light by chromatophores and iridophores, *Cell Tissue Res.* 329 (2007) 179–186, <https://doi.org/10.1007/s00441-007-0384-8>.
- [6] R.A. Cloney, S.L. Brocco, Chromatophore organs, reflector cells, iridocytes and leucophores in cephalopods, *Integr. Comp. Biol.* 23 (1983) 581–592, <https://doi.org/10.1093/icb/23.3.581>.
- [7] A. Chatterjee, B. Norton-Baker, L.E. Bagge, P. Patel, A.A. Gorodetsky, An introduction to color-changing systems from the cephalopod protein reflectin, *Bioinspiration Biomimetics* 13 (2018) 1–10, <https://doi.org/10.1088/1748-3190/aab804>.
- [8] M.J. How, M.D. Norman, J. Finn, W.S. Chung, N.J. Marshall, Dynamic skin patterns in cephalopods, *Front. Physiol.* 8 (2017) 1–13, <https://doi.org/10.3389/fphys.2017.00393>.
- [9] W.J. Crookes, L.L. Ding, Q.L. Huang, J.R. Kimbell, J. Horwitz, M.J. McFall-Ngai, Reflectins: the unusual proteins of squid reflective tissues, *Science* 303 (2004) 235–238, <https://doi.org/10.1126/science.1091288>, 1979.
- [10] L.M. Mäthger, S.L. Senft, M. Gao, S. Karaveli, G.R.R. Bell, R. Zia, A.M. Kuzirian, P. B. Dennis, W.J. Crookes-Goodson, R.R. Naik, G.W. Kattawar, R.T. Hanlon, Bright white scattering from protein spheres in color changing, flexible cuttlefish skin, *Adv. Funct. Mater.* 23 (2013) 3980–3989, <https://doi.org/10.1002/adfm.201203705>.
- [11] D.G. DeMartini, D.V. Krogstad, D.E. Morse, Membrane invaginations facilitate reversible water flux driving tunable iridescence in a dynamic biophotonic system, *Proc. Natl. Acad. Sci. USA* 110 (2013) 2552–2556, <https://doi.org/10.1073/pnas.1217260110>.
- [12] D.G. DeMartini, M. Izumi, A.T. Weaver, E. Pandolfi, D.E. Morse, Structures, organization, and function of reflectin proteins in dynamically tunable reflective cells, *J. Biol. Chem.* 290 (2015) 15238–15249, <https://doi.org/10.1074/jbc.M115.638254>.
- [13] R.T. Hanlon, L.M. Mathger, G.R.R. Bell, A.M. Kuzirian, S.L. Senft, White reflection from cuttlefish skin leucophores, *Bioinspiration Biomimetics* 13 (2017) 2–28, <https://doi.org/10.1088/1748-3190/aaa3a9>.
- [14] A. Ghoshal, D.G. DeMartini, E. Eck, D.E. Morse, Optical parameters of the tunable Bragg reflectors in squid, *J. R. Soc. Interface* 10 (2013) 19–23, <https://doi.org/10.1098/rsif.2013.0386>.

- [15] A.R. Tao, D.G. DeMartini, M. Izumi, A.M. Sweeney, A.L. Holt, D.E. Morse, The role of protein assembly in dynamically tunable bio-optical tissues, *Biomaterials* 31 (2010) 793–801, <https://doi.org/10.1016/j.biomaterials.2009.10.038>.
- [16] M. Izumi, A.M. Sweeney, D. DeMartini, J.C. Weaver, M.L. Powers, A. Tao, T. V. Silvas, R.M. Kramer, W.J. Crookes-Goodson, L.M. Mäthger, R.R. Naik, R. T. Hanlon, D.E. Morse, Changes in reflectin protein phosphorylation are associated with dynamic iridescence in squid, *J. R. Soc. Interface* 7 (2010) 549–560, <https://doi.org/10.1098/rsif.2009.0299>.
- [17] L. Phan, D.D. Ordinario, E. Karshalev, W.G. Walkup IV, M.A. Shenk, A. A. Gorodetsky, Infrared invisibility stickers inspired by cephalopods, *J Mater Chem C Mater* 3 (2015) 6493–6498, <https://doi.org/10.1039/c5tc00125k>.
- [18] R. Kautz, D.D. Ordinario, V. Tyagi, P. Patel, T.N. Nguyen, A.A. Gorodetsky, Cephalopod-derived biopolymers for ionic and protonic transistors, *Adv. Mater.* 30 (2018) 1704917, <https://doi.org/10.1002/adma.201704917>.
- [19] L.F. Deravi, A.P. Magyar, S.P. Sheehy, G.R.R. Bell, L.M. Mäthger, S.L. Senft, T. J. Wardill, W.S. Lane, A.M. Kuzirian, R.T. Hanlon, E.L. Hu, K.K. Parker, The structure-function relationships of a natural nanoscale photonic device in cuttlefish chromatophores, *J. R. Soc. Interface* 11 (2014) 20130942, <https://doi.org/10.1098/rsif.2013.0942>.
- [20] R. Levenson, D.G. Demartini, D.E. Morse, R. Levenson, D.G. Demartini, D. E. Morse, Molecular mechanism of reflectin's tunable biophotonic control : opportunities and limitations for new optoelectronics, *APL Mater.* 5 (2017) 1–11, <https://doi.org/10.1063/1.4985758>.
- [21] R. Levenson, C. Bracken, C. Sharma, J. Santos, C. Arata, B. Malady, D.E. Morse, Calibration between trigger and color: neutralization of a genetically encoded coulombic switch and dynamic arrest precisely tune reflectin assembly, *J. Biol. Chem.* 294 (2019) 16804–16815, <https://doi.org/10.1074/jbc.RA119.010339>.
- [22] R. Levenson, C. Bracken, N. Bush, D.E. Morse, Cyclable condensation and hierarchical assembly of metastable reflectin proteins, the drivers of tunable biophotonics, *J. Biol. Chem.* 291 (2016) 4058–4068, <https://doi.org/10.1074/jbc.M115.686014>.
- [23] R. Levenson, B. Malady, T. Lee, Y. Al Sabeh, M.J. Gordon, D.E. Morse, Protein charge neutralization is the proximate driver dynamically tuning reflectin assembly, *Int. J. Mol. Sci.* 25 (2024) 8954, <https://doi.org/10.3390/ijms25168954>.
- [24] T.-C. Huang, R. Levenson, Y. Li, P. Kohl, D.E. Morse, M.S. Shell, M.E. Helgeson, A colloidal model for the equilibrium assembly and liquid-liquid phase separation of the reflectin A1 protein, *Biophys. J.* 123 (2024) 3065–3079, <https://doi.org/10.1016/j.bpj.2024.07.004>.
- [25] I. Lychko, C.L. Soares, A.J.M. Barbosa, T.R. Calmeiro, R.F. de P. Martins, A.M.G. C. Dias, A.C.A. Roque, Kinetics of charge-dependent reversible condensation of reflectin nanostructures, *Mater Adv* 6 (2025) 157–167, <https://doi.org/10.1039/D4MA00788C>.
- [26] D.D. Ordinario, E.M. Leung, L. Phan, R. Kautz, W.K. Lee, M. Naeim, J.P. Kerr, M. J. Aquino, P.E. Sheehan, A.A. Gorodetsky, Protonic devices from a cephalopod structural protein, *Adv. Opt. Mater.* 5 (2017) 1600751, <https://doi.org/10.1002/adom.201600751>.
- [27] K.L. Naughton, L. Phan, E.M. Leung, R. Kautz, Q. Lin, Y. Van Dyke, B. Marmioli, B. Sartori, A. Arvai, S. Li, M.E. Pique, M. Naeim, J.P. Kerr, M.J. Aquino, V. A. Roberts, E.D. Getzoff, C. Zhu, S. Bernstorff, A.A. Gorodetsky, Self-assembly of the cephalopod protein reflectin, *Adv. Mater.* 28 (2016) 8405–8412, <https://doi.org/10.1002/adma.201601666>.
- [28] R.M. Kramer, W.J. Crookes-Goodson, R.R. Naik, The self-organizing properties of squid reflectin protein, *Nat. Mater.* 6 (2007) 533–538, <https://doi.org/10.1038/nmat1930>.
- [29] J.J. Loke, S. Hoon, A. Miserez, Cephalopod-mimetic tunable photonic coatings assembled from quasi-monodispersed reflectin protein nanoparticles, *ACS Appl. Mater. Interfaces* 14 (2022) 21436–21452, <https://doi.org/10.1021/acsaami.2c01999>.
- [30] G. Qin, P.B. Dennis, Y. Zhang, X. Hu, J.E. Bressner, Z. Sun, W.J. Crookes-Goodson, R.R. Naik, F.G. Omenetto, D.L. Kaplan, Recombinant reflectin-based optical materials, *J. Polym. Sci. B Polym. Phys.* 51 (2013) 254–264, <https://doi.org/10.1002/polb.23204>.
- [31] T. Cai, K. Han, P. Yang, Z. Zhu, M. Jiang, Y. Huang, C. Xie, Reconstruction of dynamic and reversible color change using reflectin protein, *Sci. Rep.* 9 (2019) 1–11, <https://doi.org/10.1038/s41598-019-41638-8>.
- [32] Z. Guan, T. Cai, Z. Liu, Y. Dou, X. Hu, P. Zhang, X. Sun, H. Li, Y. Kuang, Q. Zhai, H. Ruan, X. Li, Z. Li, Q. Zhu, J. Mai, Q. Wang, L. Lai, J. Ji, H. Liu, B. Xia, T. Jiang, S.J. Luo, H.W. Wang, C. Xie, Origin of the reflectin gene and hierarchical assembly of its protein, *Curr. Biol.* 27 (2017) 2833–2842, <https://doi.org/10.1016/j.cub.2017.07.061>.
- [33] C.B. Albertin, O. Simakov, T. Mitros, Z.Y. Wang, J.R. Pungor, E. Edsinger-gonzales, S. Brenner, C.W. Ragsdale, D.S. Rokhsar, The octopus genome and the evolution of cephalopod neural and morphological novelties, *Nature* 524 (2015) 220–224, <https://doi.org/10.1038/nature14668>.
- [34] L. Phan, W.G. Walkup, D.D. Ordinario, E. Karshalev, J.-M. Jocson, A.M. Burke, A. A. Gorodetsky, Reconfigurable infrared camouflage coatings from a cephalopod protein, *Adv. Mater.* 25 (2013) 5621–5625, <https://doi.org/10.1002/adma.201301472>.
- [35] E. Wolde-Michael, A.D. Roberts, D.J. Heyes, A.G. Dumanli, J.J. Blaker, E. Takano, N.S. Scrutton, Design and fabrication of recombinant reflectin-based Bragg reflectors: bio-design engineering and photoisomerism induced wavelength modulation, *Sci. Rep.* 11 (2021) 14580, <https://doi.org/10.1101/2020.02.11.942110>.
- [36] D.D. Ordinario, L. Phan, W.G. Walkup IV, J.-M. Jocson, E. Karshalev, N. Hüsen, A.A. Gorodetsky, Bulk protonic conductivity in a cephalopod structural protein, *Nat. Chem.* 6 (2014) 596–602, <https://doi.org/10.1038/nchem.1960>.
- [37] A.M.G.C. Dias, C. Cena, V. Lutz-Bueno, R. Mezzenga, A. Marques, I. Ferreira, A.C. A. Roque, Solvent modulation in peptide sub-microfibers obtained by solution blow spinning, *Front. Chem.* 10 (2022) 1–9, <https://doi.org/10.3389/fchem.2022.1054347>.
- [38] D.D. Ordinario, L. Phan, W.G. Walkup IV, Y. Van Dyke, E.M. Leung, M. Nguyen, A.G. Smith, J. Kerr, M. Naeim, I. Kymissis, A.A. Gorodetsky, Production and electrical characterization of the reflectin A2 isoform from *Doryteuthis* (Loligo) pealeii, *RSC Adv.* 6 (2016) 57103–57107, <https://doi.org/10.1039/c6ra05405f>.
- [39] C. Xu, N. Kandel, X. Qiao, M.I. Khan, P. Prataksya, N.E. Tolouei, B. Chen, A. A. Gorodetsky, Long-range proton transport in films from a reflectin-derived polypeptide, *ACS Appl. Mater. Interfaces* 13 (2021) 20938–20946, <https://doi.org/10.1021/acsaami.0c18929>.
- [40] A. Chatterjee, P. Prataksya, A.L. Kwana, N. Kaimal, A.H. Cannon, B. Sartori, B. Marmioli, H. Orins, Z. Feng, S. Drake, J. Couvrette, L. Le, S. Bernstorff, Y. G. Yingling, A.A. Gorodetsky, Squid skin cell-inspired refractive index mapping of cells, vesicles, and nanostructures, *ACS Biomater. Sci. Eng.* 9 (2023) 978–990, <https://doi.org/10.1021/acsbomaterials.2c00088>.
- [41] D.D. Ordinario, L. Phan, Y. Van Dyke, T. Nguyen, A.G. Smith, M. Nguyen, N. M. Mofid, M.K. Dao, A.A. Gorodetsky, Photochemical doping of protonic transistors from a cephalopod protein, *Chem. Mater.* 28 (2016) 3703–3710, <https://doi.org/10.1021/acs.chemmater.6b00336>.
- [42] C. Xu, G.T. Stiubianu, A.A. Gorodetsky, Adaptive infrared-reflecting systems inspired by cephalopods, *Science* 359 (2018) 1495–1500, <https://doi.org/10.1126/science.aar5191>, 1979.
- [43] Y. Lu, P. Prataksya, A. Chatterjee, X. Jia, D.D. Ordinario, L. Phan, J.A. Cerna Sanchez, R. Kautz, V. Tyagi, P. Patel, Y. Van Dyke, M.K. Dao, J.P. Kerr, J. Long, A. Allevato, J. Leal-Cruz, E. Tseng, E.R. Peng, A. Reuter, J. Couvrette, S. Drake, F. G. Omenetto, A.A. Gorodetsky, Proton conduction in inkjet-printed reflectin films, *APL Mater.* 8 (2020) 101113, <https://doi.org/10.1063/5.0019552>.
- [44] Z. Wang, C. Wang, H. Hou, W. Liu, R. Nian, H. Sun, X. Chen, G. Cui, A facile fabrication of stimulus-responsive amorphous photonic crystals in the near-infrared region, *Appl. Surf. Sci.* 479 (2019) 1014–1020, <https://doi.org/10.1016/j.apsusc.2019.02.143>.
- [45] D.D. Ordinario, L. Phan, J.M. Jocson, T. Nguyen, A.A. Gorodetsky, Protonic transistors from thin reflectin films, *APL Mater.* 3 (2015) 1–6, <https://doi.org/10.1063/1.4901296>.
- [46] L. Phan, R. Kautz, J. Arulmoli, I.H. Kim, D.T.T. Le, M.A. Shenk, M.M. Pathak, L. A. Flanagan, F. Tombola, A.A. Gorodetsky, Reflectin as a material for neural stem cell growth, *ACS Appl. Mater. Interfaces* 8 (2016) 278–284, <https://doi.org/10.1021/acsaami.5b08717>.
- [47] P.B. Dennis, K.M. Singh, M.C. Vasudev, R.R. Naik, W.J. Crookes-Goodson, Research Update: a minimal region of squid reflectin for vapor-induced light scattering, *APL Mater.* 5 (2017) 120701, <https://doi.org/10.1063/1.4997199>.
- [48] G. Bogdanov, A. Chatterjee, N. Makeeva, A. Farrukh, A.A. Gorodetsky, Squid leucophore-inspired optical engineering of human cells, *iScience* 26 (2023) 106854, <https://doi.org/10.1016/j.isci.2023.106854>.
- [49] A. Chatterjee, J.A. Cerna Sanchez, T. Yamauchi, V. Taupin, J. Couvrette, A. A. Gorodetsky, Cephalopod-inspired optical engineering of human cells, *Nat. Commun.* 11 (2020) 1–13, <https://doi.org/10.1038/s41467-020-16151-6>.
- [50] I. Lychko, C.L. Soares, A.M.G.C. Dias, A.C.A. Roque, A scalable method to purify reflectins from inclusion bodies, *Sep. Purif. Technol.* 315 (2023) 123736, <https://doi.org/10.1016/j.seppur.2023.123736>.
- [51] M.J. Umerani, P. Prataksya, A. Chatterjee, J.A. Cerna Sanchez, H.S. Kim, G. Ilc, M. Kovacic, C. Magnan, B. Marmioli, B. Sartori, A.L. Kwana, H. Orins, A. W. Bartlett, E.M. Leung, Z. Feng, K.L. Naughton, B. Norton-Baker, L. Phan, J. Long, A. Allevato, J.E. Leal-Cruz, Q. Lin, P. Baldi, S. Bernstorff, J. Plavec, Y. G. Yingling, A.A. Gorodetsky, Structure, self-assembly, and properties of a truncated reflectin variant, *Proc. Natl. Acad. Sci. U. S. A.* 117 (2021) 32891–32901, <https://doi.org/10.1073/PNAS.2009044117>.
- [52] M. Belcald, G. Casaburi, S.J. McAnulty, H. Schmidbaur, A.M. Suria, S. Moriano-Gutierrez, M. Sabrina Pankey, T.H. Oakley, N. Kremer, E.J. Koch, A.J. Collins, H. Nguyen, S. Lek, I. Goncharenko-Foster, P. Minx, E. Sodergren, G. Weinstock, D. S. Rokhsar, M. McFall-Ngai, O. Simakov, J.S. Foster, S.V. Nyholm, Symbiotic organs shaped by distinct modes of genome evolution in cephalopods, *Proc. Natl. Acad. Sci. U. S. A.* 116 (2019) 3030–3035, <https://doi.org/10.1073/pnas.1817322116>.
- [53] A.M.G.C. Dias, I.P. Moreira, I. Lychko, C. Lopes Soares, A. Nurrito, A.J. Moura Barbosa, V. Lutz-Bueno, R. Mezzenga, A.L. Carvalho, A.S. Pina, A.C.A. Roque, Hierarchical self-assembly of a reflectin-derived peptide, *Front. Chem.* 11 (2023) 1267563, <https://doi.org/10.3389/fchem.2023.1267563>.
- [54] P.Y. Liu, L.K. Chin, W. Ser, H.F. Chen, C.M. Hsieh, C.H. Lee, K.B. Sung, T.C. Aiy, P. H. Yap, B. Liedberg, K. Wang, T. Bourouina, Y. Leprince-Wang, Cell refractive index for cell biology and disease diagnosis: past, present and future, *Lab Chip* 16 (2016) 634–644, <https://doi.org/10.1039/c5lc01445j>.
- [55] M. Roscin, A. Herrel, P. Zaharias, R. Cornette, V. Fernandez, I. Kruta, Y. Cherel, I. Rouget, Every hooked beak is maintained by a prey: ecological signal in cephalopod beak shape, *Funct. Ecol.* 36 (2022) 2015–2028, <https://doi.org/10.1111/1365-2435.14098>.
- [56] A. Miserez, Y. Li, J.H. Waite, F. Zok, Jumbo squid beaks: inspiration for design of robust organic composites, *Acta Biomater.* 3 (2007) 139–149, <https://doi.org/10.1016/j.actbio.2006.09.004>.
- [57] Y. Tan, S. Hoon, P.A. Guerette, W. Wei, A. Ghadban, C. Hao, A. Miserez, J. H. Waite, Infiltration of chitin by protein coacervates defines the squid beak

- mechanical gradient, *Nat. Chem. Biol.* 11 (2015) 488–495, <https://doi.org/10.1038/nchembio.1833>.
- [58] A. Miserez, D. Rubin, J.H. Waite, Cross-linking chemistry of squid beak, *J. Biol. Chem.* 285 (2010) 38115–38124, <https://doi.org/10.1074/jbc.M110.161174>.
- [59] A. Miserez, T. Schneeberk, C. Sun, F.W. Zok, J.H. Waite, The transition from stiff to compliant materials in squid beaks, *Science* 319 (2008) 1816–1819, <https://doi.org/10.1126/science.1154117>, 1979.
- [60] B. Gabryelczyk, H. Cai, X. Shi, Y. Sun, P.J.M. Swinkels, S. Salentini, K. Pervushin, A. Miserez, Hydrogen bond guidance and aromatic stacking drive liquid-liquid phase separation of intrinsically disordered histidine-rich peptides, *Nat. Commun.* 10 (2019) 5465, <https://doi.org/10.1038/s41467-019-13469-8>.
- [61] C.B. Albertin, S. Medina-Ruiz, T. Mitros, H. Schmidbaur, G. Sanchez, Z.Y. Wang, J. Grimwood, J.J.C. Rosenthal, C.W. Ragsdale, O. Simakov, D.S. Rokhsar, Genome and transcriptome mechanisms driving cephalopod evolution, *Nat. Commun.* 13 (2022) 2427, <https://doi.org/10.1038/s41467-022-29748-w>.
- [62] D. Thakur, A. Bairwa, B. Dipta, P. Jhilla, A. Chauhan, An overview of fungal chitinases and their potential applications, *Protoplasma* 260 (2023) 1031–1046, <https://doi.org/10.1007/s00709-023-01839-5>.
- [63] M.B. Howard, N.A. Ekborg, R.M. Weiner, S.W. Hutcheson, Detection and characterization of chitinases and other chitin-modifying enzymes, *J. Ind. Microbiol. Biotechnol.* 30 (2003) 627–635, <https://doi.org/10.1007/s10295-003-0096-3>.
- [64] J.R. Devlin, J. Behnsen, Bacterial chitinases and their role in human infection, *Infect. Immun.* 91 (2023), <https://doi.org/10.1128/iai.00549-22>.
- [65] H. Cai, B. Gabryelczyk, M.S.S. Manimekalai, G. Grüber, S. Salentini, A. Miserez, Self-coacervation of modular squid beak proteins—a comparative study, *Soft Matter* 13 (2017) 7740–7752, <https://doi.org/10.1039/c7sm01352c>.
- [66] K. Suyama, M. Mawatari, D. Tatsubo, I. Maeda, T. Nose, Simple regulation of the self-assembling ability by multimerization of elastin-derived peptide (FPGVG) nUsing nitrilotriacetic acid as a building block, *ACS Omega* 6 (2021) 5705–5716, <https://doi.org/10.1021/acsomega.0c06140>.
- [67] M.B. Linder, Biomaterials: recipe for squid beak, *Nat. Chem. Biol.* 11 (2015) 455–456, <https://doi.org/10.1038/nchembio.1842>.
- [68] Y. Tan, S. Hoon, P.A. Guerette, W. Wei, A. Ghabban, C. Hao, A. Miserez, J. H. Waite, Infiltration of chitin by protein coacervates defines the squid beak mechanical gradient, *Nat. Chem. Biol.* 11 (2015) 488–495, <https://doi.org/10.1038/nchembio.1833>.
- [69] Z.W. Lim, Y. Ping, A. Miserez, Glucose-responsive peptide coacervates with high encapsulation efficiency for controlled release of insulin, *Bioconjug. Chem.* 29 (2018) 2176–2180, <https://doi.org/10.1021/acs.bioconjchem.8b00369>.
- [70] Z.W. Lim, V.B. Varma, R.V. Ramanujan, A. Miserez, Magnetically responsive peptide coacervates for dual hyperthermia and chemotherapy treatments of liver cancer, *Acta Biomater.* 110 (2020) 221–230, <https://doi.org/10.1016/j.actbio.2020.04.024>.
- [71] Y. Sun, S.Y. Lau, Z.W. Lim, S.C. Chang, F. Ghadessy, A. Partridge, A. Miserez, Phase-separating peptides for direct cytosolic delivery and redox-activated release of macromolecular therapeutics, *Nat. Chem.* 14 (2022) 274–283, <https://doi.org/10.1038/s41557-021-00854-4>.
- [72] C.P. Cerrato, A. Leppert, Y. Sun, D.P. Lane, M. Arsenian-Henriksson, A. Miserez, M. Landreh, Monitoring disassembly and cargo release of phase-separated peptide coacervates with native mass spectrometry, *Anal. Chem.* 95 (2023) 10869–10872, <https://doi.org/10.1021/acs.analchem.3c02384>.
- [73] Y. Sun, X. Xu, L. Chen, W.L. Chew, Y. Ping, A. Miserez, Redox-responsive phase-separating peptide as a universal delivery vehicle for CRISPR/Cas9 genome editing machinery, *ACS Nano* 17 (2023) 16597–16606, <https://doi.org/10.1021/acsnano.3c02669>.
- [74] S. Maricar, S. Gudlur, A. Miserez, Phase-separating peptides recruiting aggregation-induced emission fluorogen for rapid *E. coli* detection, *Anal. Chem.* 95 (2023) 9924–9931, <https://doi.org/10.1021/acs.analchem.3c01046>.
- [75] B. Gabryelczyk, R. Alag, M. Philips, K. Low, A. Venkatraman, B. Kannaian, X. Shi, M. Linder, K. Pervushin, A. Miserez, In vivo liquid-liquid phase separation protects amyloidogenic and aggregation-prone peptides during overexpression in *Escherichia coli*, *Protein Sci.* 31 (2022) 4292, <https://doi.org/10.1002/pro.4292>.
- [76] A. Shebanova, Q.M. Perrin, K. Zhu, S. Gudlur, Z. Chen, Y. Sun, C. Huang, Z. W. Lim, E.A. Mondarte, R. Sun, S. Lim, J. Yu, Y. Miao, A.N. Parikh, A. Ludwig, A. Miserez, Cellular uptake of phase-separating peptide coacervates, *Adv. Sci.* 11 (2024) 2402652, <https://doi.org/10.1002/adv.202402652>.
- [77] S. Gudlur, F.V. Ferreira, J.S.M. Ting, C. Domene, S. Maricar, A.P. Le Brun, N. Yepuri, M. Moir, R. Russell, T. Darwish, A. Miserez, M. Cárdenas, pH-dependent interactions of coacervate-forming histidine-rich peptide with model lipid membranes, *Frontiers in Soft Matter* 3 (2024) 1339496, <https://doi.org/10.3389/frsfm.2023.1339496>.
- [78] H. Le Ferrand, M. Duchamp, B. Gabryelczyk, H. Cai, A. Miserez, Time-resolved observations of liquid-liquid phase separation at the nanoscale using in situ liquid transmission electron microscopy, *J. Am. Chem. Soc.* 141 (2019) 7202–7210, <https://doi.org/10.1021/jacs.9b03083>.
- [79] X. Wu, Y. Sun, J. Yu, A. Miserez, Tuning the viscoelastic properties of peptide coacervates by single amino acid mutations and salt kosmotropicity, *Commun. Chem.* 7 (2024) 5–16, <https://doi.org/10.1038/s42004-023-01094-y>.
- [80] Y. Sun, X. Wu, J. Li, M. Radiom, R. Mezzenga, C.S. Verma, J. Yu, A. Miserez, Phase-separating peptide coacervates with programmable material properties for universal intracellular delivery of macromolecules, *Nat. Commun.* 15 (2024) 10094, <https://doi.org/10.1038/s41467-024-54463-z>.
- [81] S.H. Hiew, A. Miserez, Squid sucker ring teeth: multiscale structure-property relationships, sequencing, and protein engineering of a thermoplastic biopolymer, *ACS Biomater. Sci. Eng.* 3 (2017) 680–693, <https://doi.org/10.1021/acsbiomaterials.6b00284>.
- [82] A. Miserez, J.C. Weaver, P.B. Pedersen, T. Schneeberk, R.T. Hanlon, D. Kisailus, H. Birkedal, Microstructural and biochemical characterization of the nanoporous sucker rings from *Dosidicus gigas*, *Adv. Mater.* 21 (2009) 401–406, <https://doi.org/10.1002/adma.200801197>.
- [83] P.A. Guerette, S. Hoon, D. Ding, S. Amini, A. Masic, V. Ravi, B. Venkatesh, J. C. Weaver, A. Miserez, Nanoconfined β -sheets mechanically reinforce the supra-biomolecular network of robust squid Sucker Ring Teeth, *ACS Nano* 8 (2014) 7170–7179, <https://doi.org/10.1021/nn502149u>.
- [84] D. Ding, P.A. Guerette, S. Hoon, K.W. Kong, T. Cornvik, M. Nilsson, A. Kumar, J. Lescar, A. Miserez, Biomimetic production of silk-like recombinant squid sucker ring teeth proteins, *Biomacromolecules* 15 (2014) 3278–3289, <https://doi.org/10.1021/bm500670r>.
- [85] J. Yarger, B. Cherry, A. Van Der Vaart, Uncovering the structure-function relationship in spider silk, *Nat. Rev. Mater.* 3 (2018).
- [86] M. Ramezaniaghdam, N.D. Nahdi, R. Reski, Recombinant spider silk: promises and bottlenecks, *Front. Bioeng. Biotechnol.* 10 (2022), <https://doi.org/10.3389/fbioe.2022.835637>.
- [87] D. Harvey, P. Bardelang, S.L. Goodacre, A. Cockayne, N.R. Thomas, Antibiotic spider silk: site-specific functionalization of recombinant spider silk using “click” chemistry, *Adv. Mater.* 29 (2017), <https://doi.org/10.1002/adma.201604245>.
- [88] S.H. Hiew, P.A. Guerette, O.J. Zvarec, M. Phillips, F. Zhou, H. Su, K. Pervushin, B. P. Orner, A. Miserez, Modular peptides from the thermoplastic squid sucker ring teeth form amyloid-like cross- β supramolecular networks, *Acta Biomater.* 46 (2016) 41–54, <https://doi.org/10.1016/j.actbio.2016.09.040>.
- [89] S.H. Hiew, H. Mohanram, L. Ning, J. Guo, A. Sánchez-Ferrer, X. Shi, K. Pervushin, Y. Mu, R. Mezzenga, A. Miserez, A short peptide hydrogel with high stiffness induced by 310-helices to β -sheet transition in water, *Adv. Sci.* 6 (2019) 1–11, <https://doi.org/10.1002/adv.201901173>.
- [90] D. Ding, P.A. Guerette, J. Fu, L. Zhang, S.A. Irvine, A. Miserez, From soft self-healing gels to stiff films in suckerin-based materials through modulation of crosslink density and β -sheet content, *Adv. Mater.* 27 (2015) 3953–3961, <https://doi.org/10.1002/adma.201500280>.
- [91] S. Rauscher, S. Baud, M. Miao, F.W.W. Keeley, R. Pomès, Proline and Glycine control protein self-organization into elastomeric or amyloid fibrils, *Structure* 14 (2006) 1667–1676, <https://doi.org/10.1016/j.str.2006.09.008>.
- [92] Y. Sun, F. Ding, Thermo- and pH-responsive fibrillization of squid suckerin A1H1 peptide, *Nanoscale* 12 (2020) 6307–6317, <https://doi.org/10.1039/C9NR029271D>.
- [93] S.H. Hiew, A. Sánchez-Ferrer, S. Amini, F. Zhou, J. Adamcik, P. Guerette, H. Su, R. Mezzenga, A. Miserez, Squid suckerin biomimetic peptides form amyloid-like crystals with robust mechanical properties, *Biomacromolecules* 18 (2017) 4240–4248, <https://doi.org/10.1021/acs.biomac.7b01280>.
- [94] P.A. Guerette, S. Hoon, Y. Seow, M. Rida, A. Masic, F.T. Wong, V.H.B. Ho, K. W. Kong, M.C. Demirel, A. Pena-Francesch, S. Amini, G.Z. Tay, D. Ding, A. Miserez, Accelerating the design of biomimetic materials by integrating RNA-seq with proteomics and materials science, *Nat. Biotechnol.* 31 (2013) 908–915, <https://doi.org/10.1038/nbt.2671>.
- [95] C.C. Buck, P.B. Dennis, M.K. Gupta, M.T. Grant, M.G. Crosby, J.M. Slovic, P. A. Mirau, K.A. Becknell, K.K. Comfort, R.R. Naik, Anion-mediated effects on the size and mechanical properties of enzymatically crosslinked suckerin hydrogels, *Macromol. Biosci.* 19 (2019) 1–8, <https://doi.org/10.1002/mabi.201800238>.
- [96] S.H. Hiew, J.K. Wang, K. Koh, H. Yang, A. Bacha, J. Lin, Y.S. Yip, M.I.G. Vos, L. Chen, R.M. Sobota, N.S. Tan, C.Y. Tay, A. Miserez, Bioinspired short peptide hydrogel for versatile encapsulation and controlled release of growth factor therapeutics, *Acta Biomater.* 136 (2021) 111–123, <https://doi.org/10.1016/j.actbio.2021.09.023>.
- [97] D. Ding, J. Pan, S.H. Lim, S. Amini, L. Kang, A. Miserez, Squid suckerin microneedle arrays for tunable drug release, *J. Mater. Chem. B* 5 (2017) 8467–8478, <https://doi.org/10.1039/c7tb01507k>.
- [98] Y. Ping, D. Ding, R.A.N.S. Ramos, H. Mohanram, K. Deepankumar, J. Gao, G. Tang, A. Miserez, Supramolecular β -sheets stabilized protein nanocarriers for drug delivery and gene transfection, *ACS Nano* 11 (2017) 4528–4541, <https://doi.org/10.1021/acsnano.6b08393>.
- [99] B. Cantaert, D. Ding, C. Rieu, L. Petrone, S. Hoon, K.H. Kock, A. Miserez, Stable Formation of gold nanoparticles onto redox-active solid biosubstrates made of squid suckerin proteins, *Macromol. Rapid Commun.* 36 (2015) 1877–1883, <https://doi.org/10.1002/marc.201500218>.
- [100] A. Pena-Francesch, S. Florez, H. Jung, A. Sebastian, I. Albert, W. Curtis, M. C. Demirel, Materials fabrication from native and recombinant thermoplastic squid proteins, *Adv. Funct. Mater.* 24 (2014) 7401–7409, <https://doi.org/10.1002/adfm.201401940>.
- [101] V. Latza, P.A. Guerette, D. Ding, S. Amini, A. Kumar, I. Schmidt, S. Keating, N. Oxman, J.C. Weaver, P. Fratzl, A. Miserez, A. Masic, Multi-scale thermal stability of a hard thermoplastic protein-based material, *Nat. Commun.* 6 (2015) 1–8, <https://doi.org/10.1038/ncomms9313>.
- [102] A. Pena-Francesch, H. Jung, M.A. Hickner, M. Tyagi, B.D. Allen, M.C. Demirel, Programmable proton conduction in stretchable and self-healing proteins, *Chem. Mater.* 30 (2018) 898–905, <https://doi.org/10.1021/acs.chemmater.7b04574>.
- [103] A. Pena-Francesch, H. Jung, M. Segad, R.H. Colby, B.D. Allen, M.C. Demirel, Mechanical properties of tandem-repeat proteins are governed by network defects, *ACS Biomater. Sci. Eng.* 4 (2018) 884–891, <https://doi.org/10.1021/acsbiomaterials.7b00830>.
- [104] J.A. Tomko, A. Pena-Francesch, H. Jung, M. Tyagi, B.D. Allen, M.C. Demirel, P. E. Hopkins, Tunable thermal transport and reversible thermal conductivity

- switching in topologically networked bio-inspired materials, *Nat. Nanotechnol.* 13 (2018) 959–964, <https://doi.org/10.1038/s41565-018-0227-7>.
- [105] H. Jung, A. Pena-Francesch, A. Saadat, A. Sebastian, D.H. Kim, R.F. Hamilton, I. Albert, B.D. Allen, M.C. Demirel, Molecular tandem repeat strategy for elucidating mechanical properties of high-strength proteins, *Proc. Natl. Acad. Sci. U. S. A.* 113 (2016) 6478–6483, <https://doi.org/10.1073/pnas.1521645113>.
- [106] M. Vural, A. Pena-Francesch, J. Bars-Pomes, H. Jung, H. Gudapati, C.B. Hatter, B. D. Allen, B. Anasori, I.T. Ozbolat, Y. Gogotsi, M.C. Demirel, Inkjet printing of self-assembled 2D titanium carbide and protein electrodes for stimuli-responsive electromagnetic shielding, *Adv. Funct. Mater.* 28 (2018) 1–10, <https://doi.org/10.1002/adfm.201801972>.
- [107] M. Vural, Y. Lei, A. Pena-Francesch, H. Jung, B. Allen, M. Terrones, M.C. Demirel, Programmable molecular composites of tandem proteins with graphene oxide for efficient bimorph actuators, *Carbon N Y* 118 (2017) 404–412, <https://doi.org/10.1016/j.carbon.2017.03.053>.
- [108] K. Deepankumar, C. Lim, I. Polte, B. Zappone, C. Labate, M.P. De Santo, H. Mohanram, A. Palaniappan, D.S. Hwang, A. Miserez, Supramolecular β -sheet suckerin-based underwater adhesives, *Adv. Funct. Mater.* 30 (2020) 1–11, <https://doi.org/10.1002/adfm.201907534>.
- [109] R. Ramos, K. Koh, B. Gabryelczyk, L. Chai, D. Kanagavel, X. Yan, F. Ganachaud, A. Miserez, J. Bernard, Nanocapsules produced by nanoprecipitation of designed suckerin-silk fusion proteins, *ACS Macro Lett.* 10 (2021) 628–634, <https://doi.org/10.1021/acsmacrolett.1c00171>.
- [110] A. Sánchez-Ferrer, J. Adamcik, S. Handschin, S.H. Hiew, A. Miserez, R. Mezzenga, Controlling supramolecular chiral nanostructures by self-assembly of a biomimetic β -sheet-rich amyloidogenic peptide, *ACS Nano* 12 (2018) 9152–9161, <https://doi.org/10.1021/acsnano.8b03582>.
- [111] S.H. Hiew, Y. Lu, H. Han, R.A. Gonçalves, S.R. Alfaro, R. Mezzenga, A. N. Parikh, Y. Mu, A. Miserez, Modulation of mechanical properties of short bioinspired peptide materials by single amino-acid mutations, *J. Am. Chem. Soc.* 145 (2023) 3382–3393, <https://doi.org/10.1021/jacs.2c09853>.
- [112] V. Sariola, A. Pena-Francesch, H. Jung, M. Çetinkaya, C. Pacheco, M. Sitti, M. C. Demirel, Segmented molecular design of self-healing proteinaceous materials, *Sci. Rep.* 5 (2015) 1–9, <https://doi.org/10.1038/srep13482>.
- [113] D. Gaddes, H. Jung, A. Pena-Francesch, G. Dion, S. Tadigadapa, W.J. Dressick, M. C. Demirel, Self-healing textile: enzyme encapsulated layer-by-layer structural proteins, *ACS Appl. Mater. Interfaces* 8 (2016) 20371–20378, <https://doi.org/10.1021/acsami.6b05232>.
- [114] H. Jung, C.J. Szwedkowski, A. Pena-Francesch, J.A. Tomko, B. Allen, Ş. K. Özdemir, P. Hopkins, M.C. Demirel, Ultrafast laser-probing spectroscopy for studying molecular structure of protein aggregates, *Analyst* 142 (2017) 1434–1441, <https://doi.org/10.1039/c6an02570f>.
- [115] J.M. Hershowe, W.D. Wiseman, J.E. Kath, C.C. Buck, M.K. Gupta, P.B. Dennis, R. R. Naik, M.C. Jewett, Characterizing and controlling nanoscale self-assembly of suckerin-12, *ACS Synth. Biol.* 9 (2020) 3388–3399, <https://doi.org/10.1021/acssynbio.0c00442>.
- [116] K. Koh, J.K. Wang, J.X.Y. Chen, S.H. Hiew, H.S. Cheng, B. Gabryelczyk, M.I. G. Vos, Y.S. Yip, L. Chen, R.M. Sobota, D.K.K. Chua, N.S. Tan, C.Y. Tay, A. Miserez, Squid suckerin-spider silk fusion protein hydrogel for delivery of mesenchymal stem cell secretome to chronic wounds, *Adv Healthc Mater* 12 (2023) 2201900, <https://doi.org/10.1002/adhm.202201900>.



Iana Lychko is a Postdoctoral researcher at the Biomolecular Engineering Lab at NOVA FCT. During her studies, she spent time at KTH Royal Institute of Technology and Institut des Sciences Moléculaires de Marseille, where she expanded her knowledge in peptide and protein science. She holds a PhD in Biotechnology from NOVA University of Lisbon. Currently, her work focuses on the biotechnological applications of recombinant proteins, protein engineering, and the development of stimuli-responsive biomaterials.



Inês Padrão is pursuing a PhD in Biotechnology at NOVA FCT under the supervision of Prof. Roque. Inês holds a degree in Biochemistry and a master's degree Biotechnology from NOVA FCT. Her current research interests include the study of cephalopod camouflage proteins and skin morphology.



Ana Cecília A. Roque is Full Professor in Bioengineering and head of the Biomolecular Engineering Lab at NOVA FCT. She is UCIBIO Director since 2023. Cecilia holds a degree in Chemical Engineering and a PhD in Biotechnology from Instituto Superior Técnico, and has had visiting periods at several institutions, namely University of Cambridge, University of São Paulo and KTH. Her research focus on biomimetics merging chemistry, biotechnology and engineering and, her work has been merited with several national and international distinctions. She leads the use of protein-based materials for bio-separation and biosensing, namely for artificial olfaction purposes.